JACC Vol. 48, No. 1, 2006
July 4, 2006:176–84

EPO administered 1 week after MI failed to produce the identical effect, suggesting that EPO has a time window for promotion of EPC mobilization. We found that plasma VEGF levels were elevated, peaking at 6 h after MI and returned to the baseline 1 week after MI. The EPO did not affect plasma VEGF levels. Because both VEGF and EPO are known to promote EPC mobilization in experimental conditions and are independent predictors for the number of circulating EPCs in patients with coronary heart disease (9–11,23), they may additionally or synergistically contribute to EPC mobilization. Thus, it is likely that EPO alone, at least at the dose used in the present study, might not be enough to promote CD34+MNC mobilization 1 week after MI when VEGF returns to the baseline. Although we only investigated the low dose of EPO to consider the clinical implication, it is possible that high doses of EPO would show the different results. Further investigations are needed to clarify the mechanism of EPO-stimulated EPC mobilization.

The present study also showed that EPO increased capillary-to-myocyte ratio corrected for LV hypertrophy as well as capillary density in the EPO(0) and EPO(6h) groups, suggesting that EPO promotes the neovascularization in the ischemic region. Investigators have also reported that EPO enhances neovascularization in the ischemic region in the hind-limb occlusion model (9). As suggested in the present study, EPO may enhance neovascularization via EPC mobilization. Indeed, bone marrow-derived EPCs incorporate into foci of neovascularization at the border zone of MI (12,13), and administration of ex vivo-expanded EPCs resulted in increased myocardial neovascularization (24,25). In a rat stroke model, Wang et al. (26) showed that EPO treatment, initiated 24 h after MI, enhances angiogenesis. In addition, van der Meer et al. (27) showed that capillary density was increased in the rat post-MI model even when EPO was administered 3 weeks after MI. In contrast, we showed that EPO administered 1 week after MI failed to increase capillary density. The possible explanation for this discrepancy is attributable to the different doses of EPO used. In the studies by Wang et al. (26) (5,000 IU/kg for 7 days) and van der Meer et al. (27) (8,000 IU/kg every 3 weeks), relatively high doses of EPO were administered. In contrast, in the present study, a relatively low dose (1,000 IU/kg) of EPO was administered with a single injection, and the reason for this dose in the present study is for the possible translation of our results to clinical settings more easily (6), because 8,000 or 5,000 IU/kg EPO may cause side effects. On the other hand, we noticed that a higher dose of EPO would increase capillary density and improve the cardiac function even by the late administration of EPO for clinical use.

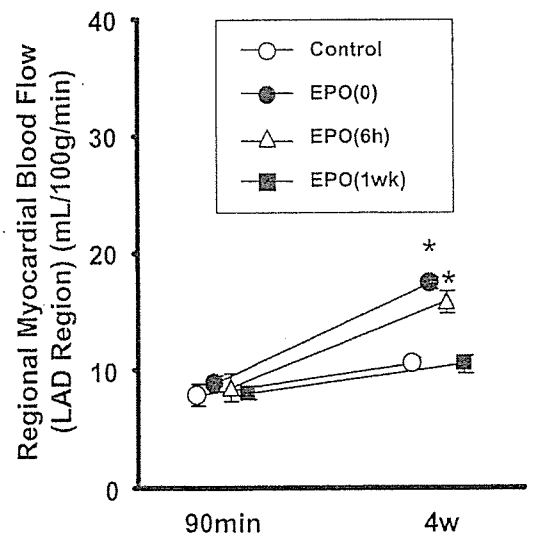

Figure 6. Regional myocardial blood flow in the ischemic (left anterior descending coronary artery [LAD]) region 90 min and 4 weeks after myocardial infarction in different experimental groups. *$p < 0.05$ versus the control group. EPO = erythropoietin.

Table 3. Time Course of Changes in Hemodynamic Parameters

Parameters	Baseline	90 Min	4 Weeks
ABP (mm Hg)			
Control	99 ± 3	101 ± 3	103 ± 2
EPO(0)	102 ± 3	99 ± 3	102 ± 2
EPO(6h)	101 ± 1	98 ± 2	101 ± 1
EPO(1wk)	102 ± 2	102 ± 3	103 ± 2
HR (per min)			
Control	131 ± 6	135 ± 6	129 ± 6
EPO(0)	128 ± 6	131 ± 3	131 ± 5
EPO(6h)	130 ± 7	135 ± 7	126 ± 6
EPO(1wk)	128 ± 6	128 ± 3	126 ± 6

Data are presented as mean ± SEM (n = 7 to 8).
ABP = arterial mean blood pressure; EPO = erythropoietin; HR = heart rate.

In the present study, MBF in the ischemic region was increased in both the EPO(0) and the EPO(6h) groups. Because neovascularization was also enhanced in these groups, increased MBF may occur secondary to the enhanced neovascularization.

The present study also showed that an administration of EPO immediately after the LAD ligation improved cardiac function at 90 min after MI, likely because of infarct size reduction, and subsequently prevented the development of cardiac dysfunction in the chronic phase. Because the previous reports showed that myocardial necrosis progresses within 6 h after the onset of MI (28,29), EPO was administered at time points of 6 h and later after LAD ligation to determine whether its activity is directed toward the acute phase of MI or the chronic phase of cardiac dysfunction. One week after MI, LVEF, LVEDD, or LVEDP was similar among the EPO(6h), EPO(1wk), and control groups. However, EPO administered 6 h, but not 1 week, after the LAD ligation improved cardiac dysfunction 4 weeks after MI when compared with the control group. Because we did not find any difference in infarct size at 4 weeks after MI between the EPO(6h) and the EPO(1wk) groups, the improvement of cardiac function in the EPO(6h) group was not attributable to the reduction of infarct size, but to the increased blood flow to the ischemic regions.

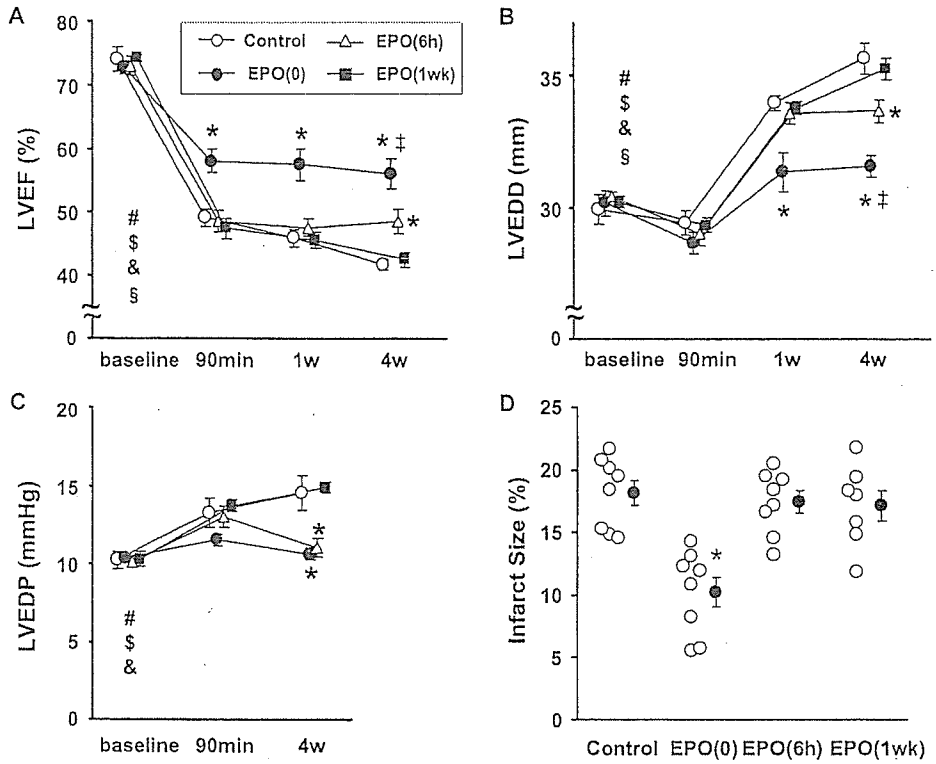

Figure 7. The time course of changes in left ventricular ejection fraction (LVEF) (A), left ventricular end-diastolic dimension (LVEDD) (B), and left ventricular end-diastolic pressure (LVEDP) (C) in different experimental groups. Statistically significant ($p < 0.05$) group-by-time interactions (analysis of variance for repeated measurements) are indicated by the following: # = all groups; $ = control × EPO(0) group; & = control × EPO(6h) group; § = EPO(0) × EPO(6h) group. (D) Infarct size at 4 weeks after myocardial infarction in different experimental groups. **Open circles** = infarct size in each animal. *$p < 0.05$ versus the control group. EPO = erythropoietin.

In conclusion, in addition to its acute effect on infarct size reduction, EPO may exert chronic cardioprotective effects through neovascularization and may be a useful adjunct for the treatment of patients with myocardial infarction.

Acknowledgments

The authors thank Hiroko Okuda, Akiko Ogai, Yoko Nagamachi, and Nobuko Kawasaki for their technical assistance.

Reprint requests and correspondence: Dr. Tetsuo Minamino, Department of Cardiovascular Medicine, Osaka University Graduate School of Medicine, 2-2 Yamadaoka, Suita, Osaka 565-0871, Japan. E-mail: minamino@medone.med.osaka-u.ac.jp.

REFERENCES

1. Krantz SB. Erythropoietin. Blood 1991;77:419–34.
2. Cotter DJ, Thamer M, Kimmel PL, Sadler JH. Secular trends in recombinant erythropoietin therapy among the U.S. hemodialysis population: 1990–1996. Kidney Int 1998;54:2129–39.
3. Sakanaka M, Wen TC, Matsuda S, et al. In vivo evidence that erythropoietin protects neurons from ischemic damage. Proc Natl Acad Sci U S A 1998;95:4635–40.
4. Chattopadhyay A, Choudhury TD, Bandyopadhyay D, Datta AG. Protective effect of erythropoietin on the oxidative damage of erythrocyte membrane by hydroxyl radical. Biochem Pharmacol 2000;59:419–25.
5. Moon C, Krawczyk M, Ahn D, et al. Erythropoietin reduces myocardial infarction and left ventricular functional decline after coronary artery ligation in rats. Proc Natl Acad Sci U S A 2003;100:11612–7.
6. Hirata A, Minamino T, Asanuma H, et al. Erythropoietin just before reperfusion reduces both lethal arrhythmias and infarct size via the phosphatidylinositol-3 kinase-dependent pathway in canine hearts. Cardiovasc Drugs Ther 2005;19:33–40.
7. Parsa CJ, Matsumoto A, Kim J, et al. A novel protective effect of erythropoietin in the infarcted heart. J Clin Invest 2003;112:999–1007.
8. Lipsic E, van der Meer P, Henning RH, et al. Timing of erythropoietin treatment for cardioprotection in ischemia/reperfusion. J Cardiovasc Pharmacol 2004;44:473–9.
9. Heeschen C, Aicher A, Lehmann R, et al. Erythropoietin is a potent physiologic stimulus for endothelial progenitor cell mobilization. Blood 2003;102:1340–6.
10. Bahlmann FH, DeGroot K, Duckert T, et al. Endothelial progenitor cell proliferation and differentiation is regulated by erythropoietin. Kidney Int 2003;64:1648–52.
11. Bahlmann FH, De Groot K, Spandau JM, et al. Erythropoietin regulates endothelial progenitor cells. Blood 2004;103:921–6.
12. Asahara T, Masuda H, Takahashi T, et al. Bone marrow origin of endothelial progenitor cells responsible for postnatal vasculogenesis in physiological and pathological neovascularization. Circ Res 1999;85:221–8.
13. Asahara T, Murohara T, Sullivan A, et al. Isolation of putative progenitor endothelial cells for angiogenesis. Science 1997;275:964–7.
14. Kitakaze M, Hori M, Morioka T, et al. Alpha 1-adrenoceptor activation mediates the infarct size-limiting effect of ischemic preconditioning through augmentation of 5'-nucleotidase activity. J Clin Invest 1994;93:2197–205.
15. Koumegawa J, Kawahara J, Kubo K, et al. Recombinant human erythropoietin corrects anemia of blood loss: a study in the dog. Int J Cell Cloning 1990;8:97–106.
16. Clifford CA, Hughes D, Beal MW, et al. Plasma vascular endothelial growth factor concentrations in healthy dogs and dogs with hemangiosarcoma. J Vet Intern Med 2001;15:131–5.
17. Horrigan MC, MacIsaac AI, Nicolini FA, et al. Reduction in myocardial infarct size by basic fibroblast growth factor after

temporary coronary occlusion in a canine model. Circulation 1996;94:1927–33.
18. Pu Q, Larouche I, Schiffrin EL. Effect of dual angiotensin converting enzyme/neutral endopeptidase inhibition, angiotensin converting enzyme inhibition, or AT1 antagonism on coronary microvasculature in spontaneously hypertensive rats. Am J Hypertens 2003;16:931–7.
19. Mori H, Haruyama S, Shinozaki Y, et al. New nonradioactive microspheres and more sensitive x-ray fluorescence to measure regional blood flow. Am J Physiol 1992;263:H1946–57.
20. Holm S. A simple sequentially rejective multiple test procedure. Scand J Stat 1979;6:65–70.
21. Shintani S, Murohara T, Ikeda H, et al. Mobilization of endothelial progenitor cells in patients with acute myocardial infarction. Circulation 2001;103:2776–9.
22. Massa M, Rosti V, Ferrario M, et al. Increased circulating hematopoietic and endothelial progenitor cells in the early phase of acute myocardial infarction. Blood 2005;105:199–206.
23. Asahara T, Takahashi T, Masuda H, et al. VEGF contributes to postnatal neovascularization by mobilizing bone marrow-derived endothelial progenitor cells. Embo J 1999;18:3964–72.
24. Kocher AA, Schuster MD, Szabolcs MJ, et al. Neovascularization of ischemic myocardium by human bone-marrow-derived angioblasts prevents cardiomyocyte apoptosis, reduces remodeling and improves cardiac function. Nat Med 2001;7:430–6.
25. Kawamoto A, Gwon HC, Iwaguro H, et al. Therapeutic potential of ex vivo expanded endothelial progenitor cells for myocardial ischemia. Circulation 2001;103:634–7.
26. Wang L, Zhang Z, Wang Y, Zhang R, Chopp M. Treatment of stroke with erythropoietin enhances neurogenesis and angiogenesis and improves neurological function in rats. Stroke 2004;35:1732–7.
27. van der Meer P, Lipsic E, Henning RH, et al. Erythropoietin induces neovascularization and improves cardiac function in rats with heart failure after myocardial infarction. J Am Coll Cardiol 2005;46:125–33.
28. Reimer KA, Lowe JE, Rasmussen MM, Jennings RB. The wavefront phenomenon of ischemic cell death. 1. Myocardial infarct size vs duration of coronary occlusion in dogs. Circulation 1977;56:786–94.
29. Hirayama A, Adachi T, Asada S, et al. Late reperfusion for acute myocardial infarction limits the dilatation of left ventricle without the reduction of infarct size. Circulation 1993;88:2565–74.

Circ J 2006; **70:** 805–809

Assessment of Genetic Effects of Polymorphisms in the MCP-1 Gene on Serum MCP-1 Levels and Myocardial Infarction in Japanese

Naoharu Iwai, MD*,**; Kazuaki Kajimoto, PhD*; Yoshihiro Kokubo, MD†; Akira Okayama, MD†; Shunichi Miyazaki, MD**; Hiroshi Nonogi, MD**; Yoichi Goto, MD**; Hitonobu Tomoike, MD†

Background Recently, the Framingham Heart Study reported that genetic variations in *CCL2* influence serum levels of monocyte chemoattractant protein-1 (MCP-1) and the incidence of myocardial infarction (MI). The purpose of the present study was to investigate the possible involvement of *CCL2* in the pathogenesis of atherosclerosis and MI in Japanese.

Methods and Results Multiple regression analysis indicated that the MCP-1 levels were significantly influenced by various factors including age, body mass index, smoking, alcohol intake, high density lipoprotein-cholesterol, and systolic blood pressure. Moreover, the serum MCP-1 level was significantly correlated with intima–media thickness ($p<0.0001$). However, this association disappeared when other clinical confounding factors were included in the analyses. Comprehensive analysis of common polymorphisms of *CCL2* in a large community-based population and in subjects with MI found that the A(–2138)T polymorphism affected the serum MCP-1 level in a subgroup of subjects 65 years and older. However, no significant differences in the frequencies of any of the polymorphisms or haplotypes were found between subjects with and without MI. None of the polymorphisms in *CCL2* affected carotid atherosclerosis.

Conclusions The serum MCP-1 level was a good surrogate marker of atherosclerosis in the present study population. Although genetic variations in *CCL2* may have some influence on MCP-1 production, their influence does not seem to contribute appreciably to atherosclerosis in Japanese. The present results did not support the recently published findings from the Framingham Heart Study. The discrepancy between the 2 studies may be related to differences in confounding factors that contribute to MCP-1 levels and in the haplotype structure of the 2 populations. (*Circ J* 2006; **70:** 805–809)

Key Words: Atherosclerosis; Epidemiology; Monocyte chemoattractant protein-1; Myocardial infarction; Polymorphisms

Monocyte chemoattractant protein-1 (MCP-1; gene name *CCL2*) has been suggested to play an important role in the initiation of atherosclerosis by recruiting monocytes to sites of injured endothelium. MCP-1 promotes monocyte differentiation to lipid-laden macrophages, and also contributes to the proliferation of arterial smooth muscle cells[1–4]

In various murine models of atherosclerosis, deletion of *CCL2* has resulted in large reductions in atherosclerotic plaque size[5] but conversely, overexpression of MCP-1 in the leukocytes of susceptible mice resulted in increased plaque size[6]

Several human epidemiological studies have also suggested links between MCP-1 levels and atherosclerotic disease[7–10] Higher MCP-1 levels have been associated with increased risks of myocardial infarction (MI), sudden death, coronary angioplasty, and stent restenosis. Very recently, the Framingham Heart Study reported that *CCL2* polymor-

(Received January 18, 2006; revised manuscript received March 13, 2006; accepted April 20, 2006)

**Department of Epidemiology, Divisions of **Cardiology and †Cardiovascular Preventive Medicine, Suita, Japan*

Mailing address: Naoharu Iwai, MD, Department of Epidemiology, Division of Cardiology, National Cardiovascular Center, 5-7-1 Fujishirodai, Suita 565-8565, Japan. E-mail: iwai@ri.ncvc.go.jp

Table 1 Characteristics of the Study Population

	Suita	*MI*	*p value*
n	2,266	342	
M (%)	46.0	87.1	<0.0001
Age	65.2 (11.0)	57.9 (9.9)	<0.0001
BMI	22.8 (3.1)	23.9 (2.9)	<0.0001
HTN (%)	38.7	53.4	<0.0001
DM (%)	9.4	40.4	<0.0001
TG	107 (71)	125 (69)*	0.0007
TC	209 (33)	197 (37)*	<0.0001
HDL-C	60 (16)	43 (13)*	<0.0001
Smoking	16.3	61.1	<0.0001
MCP-1	243 (958)**	–	
log (MCP-1)	5.23 (0.42)**	–	
IMT	0.79 (0.13)***	–	
MI	34 (1.5%)	342 (100%)	

Values are expressed as mean (SD).
**n=235, **n=2,180, ***n=2,035.*
MI, myocardial infarction; M, male subjects; BMI, body mass index (kg/m²); HTN, hypertensive subjects; DM, diabetes mellitus; TG, triglycerides (mg/dl); TC, total cholesterol (mg/dl); HDL-C, high density lipoprotein cho-lesterol (mg/dl); Smoking, current smokers; MCP-1, serum MCP-1 level (ng/ml); log (MCP-1), logarithmic transformation of MCP-1 level; IMT, intima media thickness (mm).

Table 2 Probes and Primers in TaqMan

Polymorphisms	Probe		Primer	
	VIC	FAM	Forward	Reverse
G(−2581)A	acagctGtcacttc	agacagctAtcacttc	ttccactcacttctctcacgc	gacttggccttgcatatatcaga
A(−2138)T	ctctctctaatcTgttagtgcat	ctctctctaatcAgttagtgcat	ccegaagcatgactggattat	cctaggccatctcaccctcatct
A(−1811)G	aaatggccActccatag	aatggccGctccata	caaagcagggctcgagttg	cctgggactagacttgatgtctca
C(−972)G	cttagctgtCtgcccat	ttagctgtGtgcccatt	gcctcctaactcataaatgacttagcc	ctctgtcctcagcatcttccaa
G(−928)C	aagccaGgccaactagt	ccaagccacgCaacta	tggaagatgctgaggacagaga	ggaaaacgtgtacaagtcctccaa
C(7320112)G	atgagctcttCtcttct	tgagctcttGtcttct	tgaggtataggcagaagcactgg	aagcaaaaggcaggcagga

Table 3 Summary of *CCL2* Polymorphisms

Polymorphism	Sequence	Region		Mi-AF
G(−2581)A	GACAGCT[G/A]TCACTTT	Promoter		0.332
G(−2411)C	CAAAGCT[G/C]GGAAGTT	Promoter		0.082
A(−2138)T	CACTAAC[T/A]GATTAGA	Promoter		0.049
A(−1811)T	AATGGCC[A/T]CTCCATA	Promoter		0.082
C(−972)G	TAGCTGT[C/G]TGCCCAT	Promoter		0.005
G(−928)C	CCAAGCA[G/C]GCAACTA	Promoter		0.049
C(−362)G	CGCTTCA[C/G]AGAAAGC	Promoter		0.332
C(7320112)G	GCTCTTT[C/G]TCTTCTC	Intron1		0.086
T(7320249)C	CCTGCTG[T/C]TATAACT	Exon2	Cys−>Cys	0.044
C(7320891)T	AGACACC[C/T]TGTTTTA	Exon3	3'−UTR	0.332

Mi-AF (minor allele frequency) was calculated based on the sequencing data of 93 subjects.

phisms are associated with serum MCP-1 levels and MI.[11] In genetic association studies, validation in other study populations is very important to confirm that the observed effects are not statistical errors, so the purpose of the present study was to assess the genetic effects of *CCL2* polymorphisms on serum MCP-1 levels and atherosclerosis in Japanese subjects.

Methods

Study Population

The selection criteria and design of the Suita study have been described previously.[12–14] The genotypes were determined in 2,266 subjects (including 34 MI subjects) recruited from the Suita study between September 2003 and March 2005. Serum MCP-1 levels were measured in 2,180 subjects. The MI group consisted of 342 randomly selected inpatients and outpatients with documented MI who were enrolled in the Division of Cardiology at the National Cardiovascular Center between May 2001 and April 2003.[15,16] All the subjects enrolled in the present study gave written informed consent. The present study was approved by the Ethics Committee of the National Cardiovascular Center and by the Committee on Genetic Analysis and Gene Therapy of the National Cardiovascular Center. The characteristics of the study population are shown in Table 1. Subjects with systolic blood pressure (SBP) ≥140 mmHg, diastolic blood pressure ≥90 mmHg, and/or who were taking antihypertensive medication were categorized as having hypertension. Subject with fasting blood glucose ≥126 mg/dl, hemoglobin A1c ≥6.5%, and/or who were being treated for diabetes mellitus was categorized as having the disease.

Fasting serum samples were collected and stored at −80°C. MCP-1 levels were measured in duplicate with a commercially available ELISA kit (R&D Systems, Minneapolis, MN, USA) according to the manufacturer's instructions. The inter- and intra-assay variabilities were 6.3% and 6.2%, respectively. Because the distribution of serum MCP-1 levels was skewed, the values were logarithmically transformed in the statistical analysis.

The details of the method used for the carotid ultrasonic examination have been reported previously.[14] We used a high-resolution B-mode ultrasonic machine with 7.5-MHz transducers, which gave an axial resolution of 0.2 mm. The regions between 30 mm proximal from the beginning of the dilation of the bifurcation bulb and 15 mm distal from the flow divider of both common carotid arteries (CCAs) were scanned. All measurements were made at the time of scanning with the instrument's electronic caliper and were recorded as photocopies. The intima–media thickness (IMT) was measured on a longitudinal scan of the CCA at a point 10 mm proximal from the beginning of the dilation of the bulb.

DNA Study

The promoter (up to −2.8 kb) and exons 1, 2, and 3 (including 3'UTR) regions were sequenced in 93 subjects, which included the top 12 subjects with high serum MCP-1 levels and the bottom 12 subjects with low serum MCP-1 levels. The sequence primers will be provided on request. The genotypes were determined by the TaqMan method (Table 2). The success rate of genotyping was greater than 96%.

Statistical Analysis

Values are expressed as mean ± standard deviation (SD). All statistical analyses were performed with the JMP statistical package (SAS Institute Inc, Cary, NC, USA). Multiple regression analysis was performed to obtain predictors of the serum MCP-1 level and to assess the contribution of polymorphisms of *CCL2* to the serum MCP-1 level. Multiple logistic analysis was performed to obtain predictors for MI. Residuals of the serum MCP-1 level and IMT were calculated by adjusting for appropriate confounding factors. R-square values between polymorphisms and haplotype frequencies in the control and MI groups were analyzed using the SNPAlyze Pro statistical package (version 3.2, Dynacom Inc). A statistical power calculation was per-

Table 4 Linkage Disequilibrium Among the Polymorphisms of *CCL2*

	G(−2581)A	A(−2138)T	A(−1811)T	C(−972)G	G(−928)C	C(7320112)G
G(−2581)A						
A(−2138)T	0.12356					
A(−1811)T	0.16035	0.00565				
C(−972)G	0.02467	0.00086	0.00034			
G(−928)C	0.12411	0.97084	0.00582	0.00089		
C(7320112)G	0.15605	0.00546	0.00716	0.00108	0.00562	

Linkage disequilibrium (LD) among the polymorphisms of CCL2 was calculated from the TaqMan data of the Suita subjects. R-square values between polymorphisms are shown. Tight LD was observed between the A(−2581)T and G(−928)C polymorphisms.

Table 5 Predictors of Serum MCP-1 Level

Predictor	t-ratio	p value
Age	7.9	<0.0001
BMI	−3.21	0.0014
SBP	2.42	0.0155
Alcohol	2.71	0.0067
Smoking	3.36	0.0008
HDL-C	−2.59	0.0096

Predictors of serum MCP-1 levels were identified by multiple regression analysis (n=2,180). Alcohol, ethanol consumption per day (g/day); Smoking, number of cigarettes per day X years.
SBP, systolic blood pressure. See Table 1 for other abbreviations.

Table 6 Predictors of Intima-Media Thickness

Predictor	t-ratio	p value
log (MCP-1)	0.13	0.7191
Age	353.82	<0.0001
SBP	29.67	<0.0001
Sex	33.21	<0.0001
BMI	33.45	<0.0001

n=2,034, F=128.197, p<0.0001.
The serum MCP-1 levels were assessed in 2,034 of the 2,035 subjects assessed by carotid sonography.
See Tables 1,5 for abbreviations.

Table 7 Influence of the Polymorphisms of *CCL2* on Serum MCP-1 Level

	AA	Aa	aa	p value
G(−2581)A	0.002 (0.399)	0.004 (0.418)	−0.020 (0.387)	0.692
n	936	961	270	
A(−2138)T	−0.006 (0.402)	0.049 (0.436)	−0.054 (0.211)	0.122 (0.052)
n	1,909	253	7	
A(−1811)T	0.006 (0.407)	−0.031 (0.406)	−0.079 (0.292)	0.268 (0.117)
n	1,839	313	13	
C(−972)G	−0.001 (0.406)	0.045 (0.404)	–	0.409
n	2,111	54		
G(−928)C	−0.006 (0.403)	0.048 (0.430)	−0.054 (0.211)	0.123 (0.052)
n	1,896	262	7	
C(7320112)G	0.004 (0.401)	−0.013 (0.023)	−0.163 (0.108)	0.259 (0.349)
	1,840	311	14	
A(−2138)T	−0.012 (0.351)	0.081 (0.462)	−0.051 (0.153)	0.0126 (0.0041)
Age ≥65 years	1,041	154	4	
G(−928)C	−0.012 (0.351)	0.081 (0.500)	−0.051 (0.153)	0.0124 (0.0040)
Age ≥65 years	1,035	156	4	

Residuals of log (MCP-1) were calculated by adjusting for Age, BMI, SBP, alcohol, smoking, and HDL-C. Values are expressed as mean (SD). p values calculated by grouping AA/Aa+aa are shown in parentheses. The effects of the A(−2138)T and G(−928)C polymorphisms on the MCP-1 level were more significant in subjects aged 65 years and older.
See Tables 1,5 for abbreviations.

formed with the statistical package SamplePower (version 2.0, SPSS, Chicago, IL, USA).

Results

Sequence Analysis of CCL2

Sequence analyses in 93 subjects revealed the existence of 10 polymorphisms (Table 3) of *CCL2*. The G(−2581)A was in almost complete linkage disequilibrium (LD) with the C(−362)G and C(7320891)T polymorphisms. The A(−1811)G polymorphism was in almost complete LD with the G(−2411)C polymorphism. Thus, the genotypes of the C(−362)G, C(7320891)T, and G(−2411)C polymorphisms were not determined in the present study. Because the polymorphism in exon 2 [T(7320249)C] was synonymous (Cys−>Cys), this polymorphism was also not determined in the present study. The genotypes of the remaining 6 polymorphisms were determined by the TaqMan method in a total of 2,570 subjects. The LD values calculated from R-square values among these SNPs are shown in Table 4.

Clinical Correlates of Serum MCP-1 Level

Multiple regression analysis indicated that the MCP-1 level was significantly influenced by various factors (p< 0.0001, R-square=0.054) including age (p<0.0001), body mass index (BMI; p=0.0014), smoking (p=0.0008), alcohol intake (p=0.0067), high-density lipoprotein cholesterol (p=0.0096), and SBP (p=0.0155) (Table 5).

Many studies have reported that the serum MCP-1 level is an excellent indicator of atherosclerosis and in our study population the serum MCP-1 level significantly correlated with IMT (p<0.0001, R-square=0.009). However, this association disappeared when other clinical confounding factors were included in the multiple regression analyses (Table 6).

Table 8 *CCL2* Polymorphisms and Incidence of MI

	MI (−)			MI			p value
	AA	Aa	aa	AA	Aa	aa	
G(−2581)A (%)	946 (43.35)	966 (44.13)	274 (12.52)	149 (40.93)	176 (48.53)	39 (10.71)	0.2857
A(−2138)T (%)	1,931 (88.25)	250 (11.43)	7 (0.32)	218 (87.36)	45 (12.36)	1 (0.27)	0.8686 [0.6289]
A(−1811)T (%)	1,861 (85.02)	314 (14.34)	14 (0.64)	304 (83.29)	56 (15.34)	5 (1.37)	0.3337 [0.3999]
C(−972)G (%)	2,130 (97.53)	54 (2.47)		357 (98.08)	7 (1.92)		0.5548
G(−928)C (%)	1,918 (87.82)	259 (11.86)	7 (0.32)	319 (87.40)	45 (12.33)	1 (0.27)	0.9578 [0.8200]
C(7320112)G (%)	1,855 (84.94)	315 (14.42)	14 (0.64)	302 (82.74)	61 (16.71)	2 (0.55)	0.5229 [0.2880]

Genotype frequencies between subjects with and without MI are shown. p values calculated by grouping AA/Aa + aa are shown in square parentheses.
See Table 1 for abbreviation.

Table 9 Influence of *CCL2* Polymorphisms on IMT

	AA	Aa	aa	p value
G(−2581)A	−0.003 (0.104)	0.001 (0.105)	0.006 (0.115)	0.421
n	865	908	255	
A(−2138)T	0.000 (0.106)	−0.001 (0.103)	0.065 (0.118)	0.319
n	1,784	237	6	(0.958)
A(−1811)T	0.000 (0.105)	0.003 (0.112)	−0.049 (0.068)	0.227
n	1,717	294	12	(0.752)
C(−972)G	0.000 (0.106)	0.000 (0.113)	–	0.964
n	1,970	53		
G(−928)C	0.000 (0.106)	−0.003 (0.103)	0.065 (0.118)	0.291
n	1,771	246	6	(0.802)
C(7320112)G	−0.001 (0.106)	0.005 (0.101)	0.039 (0.159)	0.275 (0.278)

Residuals of IMT were calculated by adjusting for sex, age, BMI, and SBP. Values are expressed as mean (SD). p values calculated by grouping AA/Aa + aa are shown in parentheses.
See Tables 1,5 for abbreviations.

Table 10 Haplotype Analysis of the 2 Study Populations

Suita	Framingham	G(−2581)A	A(2138)T	A(−1811)G	G(−928)C	C7320112G	MI (−)	MI	Framingham
Haplo1	H1	G	A	A	G	C	65.2	65.0	27.0
Haplo2	H4 + H5	A	A	A	G	C	13.2	10.9	26.9
Haplo3	H6	A	A	G	G	C	7.8	9.0	4.2
Haplo4	–	A	A	A	G	G	7.5	8.7	–
Haplo5	–	A	T	A	C	C	6.1	6.5	–
–	H2	A	T	A	G	G	<0.01	<0.01	20.3
–	H3	A	A	A	C	C	<0.01	<0.01	18.6

Haplotype frequencies in the MI (−) and MI groups were calculated. Haplotype frequencies reported in the Framingham study are also shown for reference.
See Table 1 for abbreviation.

Thus, the serum MCP-1 level was only a surrogate marker of atherosclerosis in the present study population.

Influence of Polymorphisms on Serum MCP-1 Level

Next, we examined the influence of polymorphisms of *CCL2* on residuals of the MCP-1 level after adjusting for the above-mentioned confounding factors (Adj-MCP1) (Table 7). Two polymorphisms, A(−2138)T and G(−928)C, tended to affect Adj-MCP1. The A(−2138)T and G(−928)C polymorphisms were in tight LD (R-square=0.97084) in this study population (Table 4). Interestingly, the influence of these polymorphisms on Adj-MCP1 seemed to be exaggerated in subjects 65 years and older whose MCP-1 levels were significantly higher than those of younger subjects.

Association Study Between CCL2 Polymorphisms and MI

No significant difference was found in the frequencies of any of the polymorphisms between the cases and controls (Table 8). Multiple logistic analyses including age and BMI indicated that none of the polymorphisms contributed to MI. Moreover, none of them affected IMT after adjusting for sex, age, SBP, and BMI (Table 9).

Haplotype Analysis

We constructed haplotypes based on the G(−2581)A, A(−2138)T, A(−1811)T, G(−928)C, and C7320112G polymorphisms and identified 5 common haplotypes that accounted for 99.7% of all haplotypes. The C(−972)G polymorphism was not included because of its low frequency. No significant difference was observed in haplotype fre-

quencies between subjects with and without MI (Table 8).

The haplotype frequencies reported in the Framingham study[11] were significantly different from those in the present study population (Table 10). Although H2 and H3, which accounted for 20.3% and 18.6%, respectively, in the Framingham study, were very rare in this study population, Haplo4 and 5, which were rare in the Framingham study, were common.

Discussion

This report describes a comprehensive analysis of the common polymorphisms of *CCL2* in both a large community-based population and subjects with MI. No significant differences in the frequencies of any of the polymorphisms were found between cases and controls. Moreover, none of the polymorphisms of *CCL2* affected carotid atherosclerosis as assessed by IMT. However, the A(−2136)T and G(−928)C polymorphisms tended to affect the serum MCP-1 level. Although genetic variations in *CCL2* may have some influence on MCP-1 production, their does not seem to contribute appreciably to atherosclerosis in Japanese subjects. Thus, our findings do not support the recently published result from the Framingham Heart Study[11] that genetic variations in *CCL2* significantly influence serum MCP-1 levels and the incidence of MI.

There may be several reasons for this discrepancy. The MCP-1 levels in the Framingham Heart Study were approximately 1.4-fold higher than those in the present study population. Genetic variation might well have an influence under a stimulated state. MCP-1 levels are influenced by various factors, as described in Table 5. It is conceivable that subjects in the Framingham Heart Study may have had higher MCP-1 levels because of stimulation by atherogenic factors that may be more prevalent in Caucasians. Indeed, the influence of genetic variations was more evident in the present study population when the analysis was limited to older subjects who had higher MCP-1 levels (Table 7).

In the Framingham Heart Study, the haplotype H2 was reported to contribute to higher MCP-1 levels, and the frequency of this haplotype was 20.3%[11] It is defined by the (−2138)T and (77320112)G genotypes, and although the A(−2138)T and G(7320112)C polymorphisms were observed in the present study population, the H2 haplotype was not ($p<0.01$%). This difference in the haplotype structure between Caucasians and Japanese might also contribute to the discrepancy between the 2 studies.

The reported positive association between the A(−2581)T polymorphism and MI in the Framingham Heart Study was based on 1,797 study subjects, including just 107 MI subjects[11] which was insufficient statistical power ($p<0.50$) to conclude that there was a positive association between the genotype and MI. Moreover, although the H2 haplotype was reported to be associated with the serum MCP-1 level, the H1 haplotype but not the H2 haplotype, was reported to be associated with MI. This inconsistency might also indicate that the Framingham study had insufficient statistical power.

Although the serum MCP-1 level is an excellent indicator of atherosclerosis[7–10] MCP-1 itself appears to make only a slight contribution to atherosclerosis (Table 6). Thus, it is unlikely that genetic polymorphisms that may only slightly influence the serum MCP-1 level will contribute significantly to the occurrence of MI and atherosclerosis. Our present findings suggest that, although genetic variations in *CCL2* may have some influence on MCP-1 production, their influence on the incidence of MI is not appreciable in Japanese. The present study also indicates the importance of clarifying the haplotype structure for comparing genetic association studies involving different ethnic backgrounds.

Acknowledgement

This study was supported by a grant from the Program for Promotion of Fundamental Studies in Health Sciences of the National Institute of Biomedical Innovation.

References

1. Yla-Herttuala S, Lipton BA, Rosenfeld ME, Sarkioja T, Yoshimura T, Leonard EJ, et al. Expression of monocyte chemoattractant protein-1 in macrophage-rich areas of human and rabbit atherosclerotic lesions. *Proc Natl Acad Sci USA* 1991; **88:** 5252–5256.
2. Yu X, Dluz S, Graves DT, Zhang L, Antoniades HN, Hollander W, et al. Elevated expression of monocyte chemoattractant protein-1 by vascular smooth muscle cells in hypercholesterolemic primates. *Proc Natl Acad Sci USA* 1992; **89:** 6953–6957.
3. Nelken NA, Coughlin SR, Gordon D, Wilcox JN. Monocyte chemoattractant protein-1 in human atheromatous plaques. *J Clin Invest* 1991; **88:** 1121–1127.
4. Viedt C, Vogel J, Athanasiou T, Shen W, Orth SR, Kubler W, et al. Monocyte chemoattractant protein-1 induces proliferation and interleukin-6 production in human smooth muscle cells by differential activation of nuclear factor-*k*B and activator protein-1. *Arterioscler Thromb Vasc Biol* 2002; **22:** 914–920.
5. Gu L, Okada Y, Clinton SK, Gerard C, Sukhova GK, Libby P, et al. Absence of monocyte chemoattractant protein-1 reduces atherosclerosis in low density lipoprotein receptor-deficient mice. *Mol Cell* 1998; **2:** 275–281.
6. Aiello RJ, Bourassa PA, Lindsey S, Weng W, Natoli E, Rollins BJ, et al. Monocyte chemoattractant protein-1 accelerates atherosclerosis in apolipoprotein E-deficient mice. *Arterioscler Thromb Vasc Biol* 1999; **19:** 1518–1525.
7. de Lemos JA, Morrow DA, Sabatine MS, Murphy SA, Gibson CM, Antman EM, et al. Association between plasma levels of monocyte chemoattractant protein-1 and long-term clinical outcomes in patients with acute coronary syndromes. *Circulation* 2003; **107:** 690–695.
8. Cipollone F, Marini M, Fazia M, Pini B, Iezzi A, Reale M, et al. Elevated circulating levels of monocyte chemoattractant protein-1 in patients with restenosis after coronary angioplasty. *Arterioscler Thromb Vasc Biol* 2001; **21:** 327–334.
9. Oshima S, Ogawa H, Hokimoto S, Nakamura S, Noda K, Saito T, et al. Plasma monocyte chemoattractant protein-1 antigen levels and the risk of restenosis after coronary stent implantation. *Jpn Circ J* 2001; **65:** 261–264.
10. Deo R, Khera A, McGuire DK, Murphy SA, de PMNJ, Morrow DA, et al. Association among plasma levels of monocyte chemoattractant protein-1, traditional cardiovascular risk factors, and subclinical atherosclerosis. *J Am Coll Cardiol* 2004; **44:** 1812–1818.
11. McDermott DH, Yang Q, Kathiresan S, Cupples LA, Massaro JM, Keaney JF Jr, et al. CCL2 polymorphisms are associated with serum monocyte chemoattractant protein-1 levels and myocardial infarction in the Framingham Heart Study. *Circulation* 2005; **112:** 1113–1120.
12. Kokubo Y, Iwai N, Tago N, Inamoto N, Okayama A, Yamawaki H, et al. Association analysis between hypertension and *CYBA*, *CLCNKB*, and *KCNMB1* functional polymorphisms in the Japanese population: The Suita study. *Circ J* 2005; **69:** 138–142.
13. Iwai N, Katsuya T, Mannami T, Higaki J, Ogihara T, Kokame K, et al. Association between SAH, an acyl-CoA synthetase gene, and hypertriglyceridemia, obesity, and hypertension. *Circulation* 2002; **105:** 41–47.
14. Mannami T, Konishi M, Baba S, Nishi N, Terao A. Prevalence of asymptomatic carotid atherosclerotic lesions detected by high-resolution ultrasonography and its relation to cardiovascular risk factors in the general population of a Japanese city: The Suita study. *Stroke* 1997; **28:** 518–525.
15. Kajimoto K, Shioji K, Ishida C, Iwanaga Y, Kokubo Y, Tomoike H, et al. Validation of the association between the gene encoding 5-lipoxygenase-activating protein and myocardial infarction in a Japanese population. *Circ J* 2005; **69:** 1029–1034.
16. Kajimoto K, Shioji K, Tago N, Tomoike H, Miyazaki S, Nonogi H, et al. Assessment of MEF2A mutations in myocardial infarction in Japanese patients. *Circ J* 2005; **69:** 1192–1195.

Available online at www.sciencedirect.com

SCIENCE DIRECT®

Life Sciences 78 (2006) 882 – 887

Life Sciences

www.elsevier.com/locate/lifescie

Vagal stimulation suppresses ischemia-induced myocardial interstitial norepinephrine release

Toru Kawada [a,*], Toji Yamazaki [b], Tsuyoshi Akiyama [b], Meihua Li [a], Hideto Ariumi [a], Hidezo Mori [b], Kenji Sunagawa [c], Masaru Sugimachi [a]

[a] *Department of Cardiovascular Dynamics, Advanced Medical Engineering Center, National Cardiovascular Center Research Institute, 5-7-1 Fujishirodai, Suita, Osaka 565-8565, Japan*

[b] *Department of Cardiac Physiology, National Cardiovascular Center Research Institute, Osaka 565-8565, Japan*

[c] *Department of Cardiovascular Medicine, Graduate School of Medical Sciences, Kyushu University, Fukuoka 812-8582, Japan*

Received 30 November 2004; accepted 31 May 2005

Abstract

Although electrical vagal stimulation exerts beneficial effects on the ischemic heart such as an antiarrhythmic effect, whether it modulates norepinephrine (NE) and acetylcholine (ACh) releases in the ischemic myocardium remains unknown. To clarify the neural modulation in the ischemic region during vagal stimulation, we examined ischemia-induced NE and ACh releases in anesthetized and vagotomized cats. In a control group (VX, $n=8$), occlusion of the left anterior descending coronary artery increased myocardial interstitial NE level from 0.46±0.09 to 83.2±17.6 nM at 30–45 min of ischemia (mean±SE). Vagal stimulation at 5 Hz (VS, $n=8$) decreased heart rate by approximately 80 beats/min during the ischemic period and suppressed the NE release to 24.4±10.6 nM ($P<0.05$ from the VX group). Fixed-rate ventricular pacing (VSP, $n=8$) abolished this vagally mediated suppression of ischemia-induced NE release. The vagal stimulation augmented ischemia-induced ACh release at 0–15 min of ischemia (VX: 11.1±2.1 vs. VS: 20.7±3.9 nM, $P<0.05$). In the VSP group, the ACh release was not augmented. In conclusion, vagal stimulation suppressed the ischemia-induced NE release and augmented the initial increase in the ACh level. These modulations of NE and ACh levels in the ischemic myocardium may contribute to the beneficial effects of vagal stimulation on the heart during acute myocardial ischemia.

Keywords: Acetylcholine; Coronary occlusion; Ventricular pacing

Introduction

Acute myocardial ischemia disrupts normal neural regulation of the heart (Armour, 1999). During prolonged ischemia, myocardial interstitial norepinephrine (NE) and acetylcholine (ACh) levels are increased in the ischemic region via local releasing mechanisms independent of efferent autonomic activities (Schömig et al., 1987; Lameris et al., 2000; Kawada et al., 2000, 2001). The excess NE release is thought to aggravate ischemic injury to the myocardium (Schömig et al., 1987). On the other hand, vagal stimulation exerts antiarrhythmic effects in the early phase of acute myocardial ischemia (Rosenshtraukh et al., 1994; Vanoli et al., 1991). A recent study from our laboratory demonstrated that vagal stimulation improved the survival rate of chronic heart failure after myocardial infarction in rats (Li et al., 2004), suggesting a long-term ameliorative effect of direct neural interventions against certain heart diseases.

With respect to electrical stimulation of the vagus, whether it alters myocardial interstitial NE and ACh levels in the ischemic region during acute myocardial ischemia remains unknown. To test the hypothesis that vagal stimulation increases the ACh level and suppresses the NE level in the ischemic region, we measured myocardial interstitial NE and ACh levels during acute myocardial ischemia in anesthetized cats using a cardiac microdialysis technique (Akiyama et al., 1991, 1994; Yamazaki et al., 1997). Effects of vagal stimulation were examined with or without fixed-rate ventricular pacing.

* Corresponding author. Tel.: +81 6 6833 5012x2427; fax: +81 6 6835 5403.
E-mail address: torukawa@res.ncvc.go.jp (T. Kawada).

0024-3205/$ - see front matter © 2005 Elsevier Inc. All rights reserved.
doi:10.1016/j.lfs.2005.05.087

Materials and methods

This investigation conforms with the *Guide for the Care and Use of Laboratory Animals* published by the US National Institutes of Health (NIH Publication No. 85-23, revised 1996).

Surgical preparation

Twenty-four adult cats weighing from 2.2 to 3.8 kg were anesthetized by an intraperitoneal injection of pentobarbital sodium (30–35 mg/kg) and ventilated mechanically with room air mixed with oxygen. The depth of anesthesia was maintained with a continuous intravenous infusion of pentobarbital sodium (1–2 mg kg^{-1} h^{-1}) through a catheter inserted from the right femoral vein to the inferior vena cava. Systemic arterial pressure (AP) was monitored from a catheter inserted from the right femoral artery into the abdominal aorta. Heart rate (HR) was determined from an electrocardiogram using a cardiotachometer. Esophageal temperature of the animal was measured using a thermometer (CTM-303, TERUMO, Japan) and was maintained at around 37 °C using a heated pad and a lamp.

Bilateral vagal nerves were sectioned through a midline cervical incision. With the animal in the lateral position, the left fifth and sixth ribs were resected to expose the heart. A dialysis probe was implanted, using a fine guiding needle, into the anterolateral free wall of the left ventricle perfused by the left anterior descending coronary artery (LAD). A 3-0 silk suture was passed around the LAD just distal to the first diagonal branch for later coronary occlusion. When an experimental protocol required electrical stimulation of the vagal efferent nerves, bipolar platinum electrodes were attached to the cardiac end of sectioned vagal nerves bilaterally. The nerves and electrodes were covered with warmed mineral oil for insulation. When an experimental protocol required cardiac pacing, bipolar stainless-steel wire electrodes were sutured at the left ventricular apex away from the implanted dialysis probe. Heparin sodium (100 U/kg) was administered intravenously to prevent blood coagulation.

In additional four anesthetized cats, the left ventricle was implanted with a dialysis probe and a pair of pacing electrodes to examine the effects of left ventricular pacing alone on the myocardial interstitial NE levels. The dialysis probe and pacing leads were placed in the same manner as described in the previous paragraph.

At the end of the experiment, the experimental animals were killed with an overdose of pentobarbital sodium. Postmortem examination confirmed that the dialysis probe had been implanted within the left ventricular myocardium.

Dialysis technique

The materials and properties of the dialysis probe have been previously described (Akiyama et al., 1991, 1994). Briefly, we designed a transverse dialysis probe. A dialysis fiber (13 mm length, 310 μm O.D., 200 μm I.D.; PAN-1200, 50,000 molecular weight cutoff, Asahi Chemical, Japan) was glued at both ends to polyethylene tubes (25 cm length, 500 μm O.D., 200 μm I.D.). The dialysis probe was perfused at a rate of 2 μl/min with Ringer solution containing the cholinesterase inhibitor eserine (100 μM). Dialysate sampling was initiated 2 h after implanting the dialysis probe, when the dialysate concentrations of NE and ACh had reached steady states (Akiyama et al., 1991, 1994). The actual dialysate sampling lagged behind a given collection period by 5 min taking into account the dead space volume between the dialysis membrane and the sample tube. Dialysate concentrations of NE and ACh were measured separately by high performance liquid chromatography with electrochemical detection (DTA-300, Eicom, Japan). Details of the NE and ACh measurements have been previously described (Akiyama et al., 1991, 1994).

Protocols

Protocol 1 (VX, n = 8)

As a control experiment, we measured ischemia-induced NE and ACh releases during 60-min LAD occlusion in vagotomized animals. After collecting a 15-min baseline dialysate sample, we occluded the LAD for 60 min and collected four consecutive 15-min dialysate samples during acute myocardial ischemia. We then loosened the LAD snare and collected a 15-min dialysate sample during reperfusion.

Protocol 2 (VS, n = 8)

We examined the effects of vagal stimulation on ischemia-induced NE and ACh releases. To avoid possible preconditioning mimetic effects of ACh released by vagal stimulation (Przyklenk and Kloner, 1995; Kawada et al., 2002a), we initiated the bilateral vagal stimulation (5 Hz, 1 ms in pulse duration and 10 V in pulse amplitude) at the onset of LAD occlusion. The vagal stimulation continued for the 60-min ischemic period and the 15-min reperfusion period.

Protocol 3 (VSP, n = 8)

To eliminate the effects of bradycardia associated with vagal stimulation, we performed vagal stimulation under fixed-rate pacing conditions. We initiated the bilateral vagal stimulation (5 Hz, 1 ms in pulse duration and 10 V in pulse amplitude) and paced the heart from the onset of LAD occlusion to the conclusion of the experimental period. The ventricular pacing rate was set close to the HR recorded immediately before the LAD occlusion.

Supplemental protocol (n = 4)

To examine the effects of left ventricular pacing on the myocardial interstitial NE levels, we collected 15-min dialysate samples under control conditions as well as under left ventricular pacing at 170 beats/min.

Statistical analysis

All data are presented as means ± SE values. In each group, the effects of LAD occlusion on dialysate concentrations of NE and ACh were examined using a repeated-measures analysis of

variance followed by a Dunnett test against respective baseline concentrations. Because the variance of NE data was very large and increased with mean, the NE data were compared after the logarithmic transform (Snedecor and Cochran, 1989). Differences were considered significant at $P<0.05$. To examine the effects of vagal stimulation with or without the ventricular pacing, dialysate concentrations of NE and ACh were compared among the three groups at each corresponding time period using one-way analysis of variance followed by a Student–Newman–Keuls test for all pairwise comparisons (Glantz, 2002). The NE data were compared after the logarithmic transform. Differences were considered significant at $P<0.05$. Heart rate and mean AP were determined immediately before the coronary occlusion (designated as time 0), after 5, 10, 15, 30, 45, and 60 min of the occlusion, and after 15 min of reperfusion. One-way analysis of variance followed by a Student–Newman–Keuls test was also applied to compare HR and mean AP among the three groups at each time point.

Results

Fig. 1 depicts LAD occlusion-induced myocardial interstitial NE accumulation within the ischemic zone. The inset shows the NE levels during baseline conditions in a magnified ordinate. In the VX group, LAD occlusion increased the NE level approximately 200 fold compared to the baseline level at 45–60 min. This occlusion-induced NE accumulation was significantly suppressed in the VS group compared with the VX group in 15–30, 30–45, and 45–60 min time periods. The difference between the VS and VX groups did not reach statistical significance at the reperfusion period. In the VSP group, in which HR was kept constant, vagal stimulation did not attenuate the occlusion-induced NE accumulation. In the supplemental protocol, the baseline myocardial interstitial NE level was 0.17±0.01 nM. The NE level during ventricular pacing at 170 beats/min was 0.21±0.09 nM.

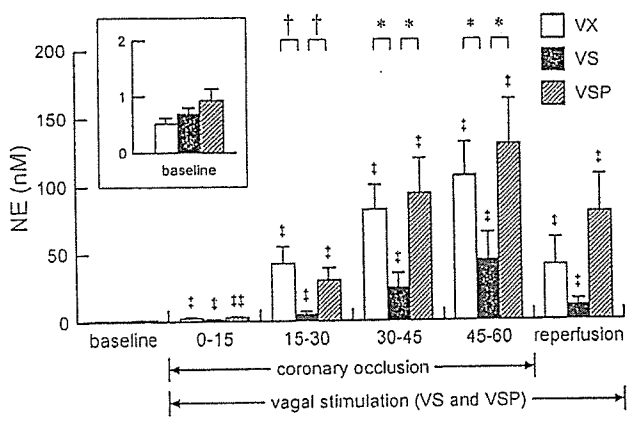

Fig. 1. Coronary occlusion-induced norepinephrine (NE) accumulation in the ischemic myocardium. VX: vagotomy, VS: vagal stimulation, VSP: vagal stimulation with ventricular pacing. The inset shows the baseline conditions with a magnified ordinate. Data are means±SE. $^{\ddagger}P<0.01$ and $^{\ddagger\ddagger}P<0.05$ from the corresponding baseline value in each group. $^{\dagger}P<0.01$ and $^{*}P<0.05$ by all pairwise comparisons among the three groups.

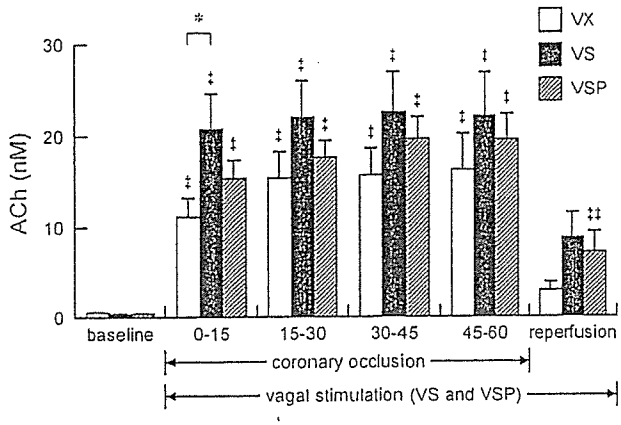

Fig. 2. Coronary occlusion-induced acetylcholine (ACh) accumulation in the ischemic myocardium. Data are means±SE. $^{\ddagger}P<0.01$ and $^{\ddagger\ddagger}P<0.05$ from the corresponding baseline value in each group. $^{*}P<0.05$ by all pairwise comparisons among the three groups.

Fig. 2 shows LAD occlusion-induced myocardial interstitial ACh accumulation within the ischemic zone. In the VX group, LAD occlusion increased the ACh level approximately 20 times higher than the baseline level at 45–60 min. The ACh level at 0–15 min was significantly higher in the VS than the VX group. For the rest of the ischemic period and reperfusion period, the differences between the VS and VX groups were not significant. The ACh levels in the VSP group did not differ from the VX group for any of the sampling periods.

Fig. 3 summarizes changes in HR and mean AP. In the VS group, HR was decreased by approximately 80 beats/min compared with the VX group at 5 min of coronary occlusion. The HR decrease continued for the rest of the ischemic period and reperfusion period. In the VSP group, HR was kept close to the preocclusion level, and it did not differ from the VX group

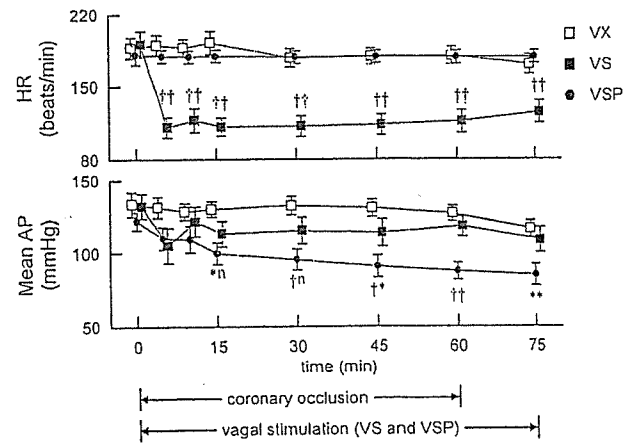

Fig. 3. Time courses of heart rate (HR) and mean arterial pressure (AP) during 60-min ischemia and 15-min reperfusion. The baseline values obtained just before coronary occlusion are plotted at time 0. Data points for VX and VSP groups are slightly displaced along the time axis for better view of overlapping points. Data are means±SE. In the HR data, †† represents statistical significance of $P<0.01$ from both the VX and VSP groups by all pairwise comparisons. In the AP data, when two characters are added to the VSP data point, the first and second characters represent the statistical significance from VX and VS groups, respectively. *, †, and n designate $P<0.05$, $P<0.01$, and "not significant", respectively.

for all the time points. Mean AP did not differ statistically between VX and VS groups. Mean AP in the VSP group progressively decreased and became significantly lower than the VX group after 15 min of the ischemic period. Mean AP in the VSP group was also significantly lower than the VS group after 45 min of the ischemic period.

Discussion

We have shown that electrical vagal stimulation suppressed ischemia-induced NE release and enhanced an initial increase in the ACh levels in the ischemic myocardium. Fixed-rate pacing abolished the suppression of ischemia-induced NE release by vagal stimulation in the present experimental settings.

Effects of vagal stimulation on ischemia-induced NE release

Several mechanisms can be put forward to explain the suppression of ischemia-induced myocardial interstitial NE release by vagal stimulation. First, activation of presynaptic muscarinic receptors on the sympathetic nerve endings inhibits the exocytotic NE release under normal physiological conditions (Levy and Blattberg, 1976). However, the presynaptic inhibition is unlikely the mechanism underlying the vagally mediated suppression of the ischemia-induced NE release because of the following reasons. Although the exocytotic release mechanism participates in the ischemia-induced NE release within the first 20 min of ischemia, the non-exocytotic release mechanism becomes predominant as the ischemic period is prolonged (Akiyama and Yamazaki, 1999). Myocardial ischemia gradually depletes ATP in the ischemic region including sympathetic nerve terminals, which leads to accumulation of axoplasmic NE and reduction of normal Na^+gradient across the plasma membrane in the sympathetic nerve terminals. The NE uptake transporter on the sympathetic nerve terminals, driven by the Na^+gradient, is then reversed, evoking non-exocytotic NE release (Schwartz, 2000). Therefore, the presynaptic inhibition of exocytotic NE release might contribute little to the suppression of ischemia-induced NE release during prolonged ischemia. Furthermore, the presynaptic inhibition of exocytotic NE release becomes less effective during the ischemic insult (Du et al., 1990; Haunstetter et al., 1994). The fact that the ischemia-induced NE release did not differ between the VSP and VX groups is also in opposition to the presynaptic inhibition as a chief mechanism underlying the vagally mediated suppression of ischemia-induced NE release (Fig. 1). Although left ventricular pacing could have affected myocardial interstitial NE levels, the results of the supplemental protocol indicates that changes in the NE levels by ventricular pacing might be negligibly small compared to the ischemia-induced NE release.

Second, the suppression of ischemia-induced NE release by vagal stimulation may be related to myocardial protection via direct vasodiation of the coronary artery. The coronary dilation may enhance collateral flow in the ischemic region and protect against myocardial deterioration evoked by ischemia. Both ACh and vasoactive intestinal polypeptide (VIP) are known to exert direct coronary dilation (Feliciano and Henning, 1998; Gross et al., 1981; Henning and Sawmiller, 2001). VIP is colocalized with ACh in the postganglionic vagal fibers and is released by high-frequency (20 Hz) vagal stimulation. VIP may interact with NE transport or exocytosis like nociceptin (Yamazaki et al., 2001). However, fixed-rate pacing abolished the ability of vagal stimulation to suppress the ischemia-induced NE release. Hence the direct coronary vasodilation and/or interaction with the sympathetic system via VIP might have played little role in suppressing ischemia-induced NE release in the present experimental settings. Another factor that should be taken into account is that the relatively low-frequency (5 Hz) stimulation might have limited the amount of VIP release from the vagal nerve endings.

Third, HR is one of the most important determinants of myocardial oxygen consumption (Mohrman and Heller, 1997). In the present study, HR in the VS group decreased to approximately 60% that of the VX group during the ischemic period (Fig. 3), which slowed the energy consumption of the myocardium. Bradycardia might also decrease ventricular contractility via a force-frequency mechanism (Maughan et al., 1985). In addition, bradycardia may increase coronary perfusion via prolongation of diastolic interval (Buck et al., 1981). These factors slowed energy consumption in the ischemic region including sympathetic nerve terminals, delaying the time course for non-exocytotic NE release. The prevention of excess NE would further reduce myocardial oxygen consumption and decelerate the progression of ischemic injury (Suga et al., 1983). The ischemia-induced NE release did not differ between the VSP and VX groups despite the lower mean AP in the VSP compared with the VX group. Although lowering AP might decrease afterload of the ventricle and reduce energy consumption, the beneficial effect of afterload reduction might have been masked in the VSP group due to inefficient cardiac pumping function associated with asynchrony between sinus rate and ventricular rate. Proper atrioventricular conduction time contributes to the ventricular filling (Meisner et al., 1985). In the VSP group, the sinus rate was reduced by vagal stimulation whereas the ventricular rate was maintained by fixed-rate pacing. Dissociation of the sinus rate and ventricular rate might have impaired the ventricular filling to a variable extent, resulting in a progressive reduction in AP.

Finally, the vagal stimulation decreases ventricular contractile force against sympathetic activation via the direct projections to the ventricle (Nakayama et al., 2001). This mechanism might have also contributed to the reduction of the myocardial oxygen consumption and slowed the progression of ischemic injury in the VS group. However, the ventricular pacing canceled the protective effects in the VSP group, possibly by the adverse influences discussed in the previous paragraph. Further studies are required to isolate the factor(s) most important for the suppression of ischemia-induced NE release by the vagal stimulation.

Effects of vagal stimulation on ischemia-induced ACh release

In contrast to the suppressive effect of NE release, vagal nerve stimulation can exert two opposing influences on ACh release in the ischemic myocardium. The nerve stimulation itself induces exocytotic ACh release from nerve endings. Acute myocardial ischemia impairs conduction of the nerves traversing in the ischemic region (Barber et al., 1983; Inoue and Zipes, 1988; Martins et al., 1989). Acute myocardial ischemia also impairs the exocytotic ACh release in the postischemic myocardium (Kawada et al., 2002b). On the other hand, acute myocardial ischemia causes myocardial ACh release in the ischemic region via a local release mechanism independent of efferent nerve activity (Kawada et al., 2000). Hence, the amount of ACh release was net effects of ACh release evoked by nerve stimulation and ischemia; vagally mediated protection against ischemic injury should augment the former and attenuate the latter.

Although vagal stimulation augmented myocardial interstitial ACh release during the 0–15 min period of coronary occlusion in the VS group than in the VX group, the initial enhancement was not observed in the VSP group. One possible mechanism for the difference in the initial ACh release between the VS and VSP groups is that the progression of ischemia in the VSP group relative to the VS group impaired the vagal nerve conduction in the ischemic region, reducing the exocytotic ACh release. The other possible mechanism is that the high levels of NE might have attenuated the stimulation-induced ACh release from the vagal nerve endings via α-adrenergic mechanisms (Akiyama and Yamazaki, 2000).

There are several limitations to the present study. First, we avoided large myocardial ischemia by occluding LAD just distal to the first diagonal branch. Accordingly, the incidence of lethal ventricular arrhythmia was too low to draw any conclusion as to the effects of vagal stimulation on the arrhythmogenesis. Further studies with larger myocardial ischemia are clearly required to examine the effects of vagal stimulation on the incidence of lethal ventricular arrhythmia in relation to the observed NE and/or ACh levels in the ischemic myocardium. Second, plasma catecolamine levels might have been increased during the LAD occlusion, which might affect HR and cardiac function in the non-ischemic region. Although changes in plasma catecholamine levels may play significant roles in determining systemic hemodynamics, the ischemic region was only poorly perfused. Accordingly, direct effects of plasma catecholamines on the myocardial interstitial NE and ACh levels in the ischemic region might have been limited in the present study.

Conclusion

Electrical vagal stimulation suppressed ischemia-induced NE release in the ischemic myocardium in anesthetized cats. The vagal stimulation augmented ischemia-induced ACh release at the 0–15 min period of ischemia. Although acute myocardial ischemia causes myocardial NE and ACh releases independent of efferent nerve activity, the vagal stimulation was able to modulate both NE and ACh levels in the ischemic region. The suppression of NE release and augmentation of initial ACh release in the ischemic myocardium by vagal stimulation may reduce the ischemic injury to the heart. The direct neural intervention could be a new modality of medical engineering to cope with ischemic heart diseases.

Acknowledgments

This study was supported by Health and Labour Sciences Research Grant for Research on Advanced Medical Technology (H14-Nano-002) from the Ministry of Health Labour and Welfare of Japan, by Grant-in-Aid for Scientific Research (C-15590786) from the Ministry of Education, Science, Sports and Culture of Japan, and by the Program for Promotion of Fundamental Studies in Health Science from the Organization for Pharmaceutical Safety and Research.

References

Akiyama, T., Yamazaki, T., 1999. Norepinephrine release from cardiac sympathetic nerve endings in the in vivo ischemic region. Journal of Cardiovascular Pharmacology 34, S11–S14.

Akiyama, T., Yamazaki, T., 2000. Adrenergic inhibition of endogenous acetylcholine release on postganglionic cardiac vagal nerve terminals. Cardiovascular Research 46, 531–538.

Akiyama, T., Yamazaki, T., Ninomiya, I., 1991. In vivo monitoring of myocardial interstitial norepinephrine by dialysis technique. American Journal of Physiology. Heart and Circulatory Physiology 261, H1643–H1647.

Akiyama, T., Yamazaki, T., Ninomiya, I., 1994. In vivo detection of endogenous acetylcholine release in cat ventricles. American Journal of Physiology. Heart and Circulatory Physiology 266, H854–H860.

Armour, J.A., 1999. Myocardial ischaemia and the cardiac nervous system. Cardiovascular Research 41, 41–54.

Barber, M.J., Mueller, T.M., Henry, D.P., Felten, S.Y., Zipes, D.P., 1983. Transmural myocardial infarction in the dog produces sympathectomy in noninfarcted myocardium. Circulation 67, 787–796.

Buck, J.D., Warltier, D.C., Hardman, H.F., Gross, G.J., 1981. Effects of sotalol and vagal stimulation on ischemic myocardial blood flow distribution in the canine heart. Journal of Pharmacological and Experimental Therapeutics 216, 347–351.

Du, X.J., Dart, A.M., Riemersma, R.A., Oliver, M.F., 1990. Failure of the cholinergic modulation of norepinephrine release during acute myocardial ischemia in the rat. Circulation Research 66, 950–956.

Feliciano, L., Henning, R.J., 1998. Vagal nerve stimulation releases vasoactive intestinal peptide which significantly increases coronary artery blood flow. Cardiovascular Research 40, 45–55.

Glantz, S.A., 2002. Primer of Biostatistics, 5th ed. McGraw-Hill, New York.

Gross, G.J., Buck, J.D., Warltier, D.C., 1981. Transmural distribution of blood flow during activation of coronary muscarinic receptors. American Journal of Physiology. Heart and Circulatory Physiology 240, H941–H946.

Haunstetter, A., Haass, M., Yi, X., Krüger, C., Kübler, W., 1994. Muscarinic inhibition of cardiac norepinephrine and neuropeptide Y release during ischemia and reperfusion. American Journal of Physiology. Regulatory, Integrative and Comparative Physiology 267, R1552–R1558.

Henning, R.J., Sawmiller, D.R., 2001. Vasoactive intestinal peptide: cardiovascular effects. Cardiovascular Research 49, 27–37.

Inoue, H., Zipes, D.P., 1988. Time course of denervation of efferent sympathetic and vagal nerves after occlusion of the coronary artery in the canine heart. Circulation Research 62, 1111–1120.

Kawada, T., Yamazaki, T., Akiyama, T., Sato, T., Shishido, T., Inagaki, M., Takaki, H., Sugimachi, M., Sunagawa, K., 2000. Differential acetylcholine release mechanisms in the ischemic and non-ischemic myocardium. Journal of Molecular and Cellular Cardiology 32, 405–414.

Kawada, T., Yamazaki, T., Akiyama, T., Inagaki, M., Shishido, T., Zheng, C., Yanagiya, Y., Sugimachi, M., Sunagawa, K., 2001. Vagosympathetic interactions in ischemia-induced myocardial norepinephrine and acetylcholine release. American Journal of Physiology. Heart and Circulatory Physiology 280, H216–H221.

Kawada, T., Yamazaki, T., Akiyama, T., Mori, H., Inagaki, M., Shishido, T., Takaki, H., Sugimachi, M., Sunagawa, K., 2002. Effects of brief ischaemia on myocardial acetylcholine and noradrenaline levels in anaesthetized cats. Autonomic Neuroscience 95, 37–42.

Kawada, T., Yamazaki, T., Akiyama, T., Mori, H., Uemura, K., Miyamoto, T., Sugimachi, M., Sunagawa, K., 2002. Disruption of vagal efferent axon and nerve terminal function in the postischemic myocardium. American Journal of Physiology. Heart and Circulatory Physiology 283, H2687–H2691.

Lameris, T.W., de Zeeuw, Sandra, Alberts, G., Boomsma, F., Duncker, D.J., Verdouw, P.D., Veld, A.J., van den Meiracker, A.H., 2000. Time course and mechanism of myocardial catecholamine release during transient ischemia in vivo. Circulation 101, 2645–2650.

Levy, M.N., Blattberg, B., 1976. Effect of vagal stimulation on the overflow of norepinephrine into the coronary sinus during cardiac sympathetic nerve stimulation in the dog. Circulation Research 38, 81–84.

Li, M., Zheng, C., Sato, T., Kawada, T., Sugimachi, M., Sunagawa, K., 2004. Vagal nerve stimulation markedly improves long-term survival after chronic heart failure in rats. Circulation 109, 120–124.

Martins, J.B., Lewis, R., Wendt, D., Lund, D.D., Schmid, P.G., 1989. Subendocardial infarction produces epicardial parasympathetic denervation in canine left ventricle. American Journal of Physiology. Heart and Circulatory Physiology 256, H859–H866.

Maughan, W.L., Sunagawa, K., Burkhoff, D., Graves, W.L. Jr., Hunter, W.C., Sagawa, K., 1985. Effect of heart rate on the canine end-systolic pressure–volume relationship. Circulation 72, 654–659.

Meisner, J.S., McQueen, D.M., Ishida, Y., Vetter, H.O., Bortolotti, U., Strom, J.A., Frater, R.W.M., Peskin, C.S., Yellin, E.L., 1985. Effects of timing of atrial systole on LV filling and mitral valve closure: computer and dog studies. American Journal of Physiology. Heart and Circulatory Physiology 249, H604–H619.

Mohrman, D.E., Heller, L.J., 1997. Cardiovascular Physiology, 4th ed. McGraw-Hill, New York, pp. 47–69.

Nakayama, Y., Miyano, H., Shishido, T., Inagaki, M., Kawada, T., Sugimachi, M., Sunagawa, K., 2001. Heart rate-independent vagal effect on end-systolic elastance of the canine left ventricule under various levels of sympathetic tone. Circulation 104, 2277–2279.

Przyklenk, K., Kloner, R.A., 1995. Low-dose i.v. acetylcholine acts as a "preconditioning-mimetic" in the canine model. Journal of Cardiac Surgery 10, 389–395.

Rosenshtraukh, L., Danilo Jr., P., Anyukhovsky, E.P., Steinberg, S.F., Rybin, V., Brittain-Valenti, K., Molina-Viamonte, V., Rosen, M.R., 1994. Mechanisms for vagal modulation of ventricular repolarization and of coronary occlusion-induced lethal arrhythmias in cats. Circulation Research 75, 722–732.

Schömig, A., Fischer, S., Kurz, T., Richardt, G., Schömig, E., 1987. Nonexocytotic release of endogenous noradrenaline in the ischemic and anoxic rat heart: mechanism and metabolic requirements. Circulation Research 60, 194–205.

Schwartz, J.H., 2000. Neurotransmitters. In: Kandel, E.R., Schwartz, J.H., Jessell, T.M. (Eds.), Principles of Neural Science, 4th ed. McGraw-Hill, New York, pp. 280–297.

Snedecor, G.W., Cochran, W.G., 1989. Statistical Methods, 8th ed. Iowa State, Iowa, pp. 290–291.

Suga, H., Hisano, R., Goto, Y., Yamada, O., Igarashi, Y., 1983. Effect of positive inotropic agents on the relation between oxygen consumption and systolic pressure volume area in canine left ventricle. Circulation Research 53, 306–318.

Vanoli, E., De Ferrari, G.M., Stramba-Badiale, M., Hull Jr., S.S., Foreman, R.D., Schwartz, P.J., 1991. Vagal stimulation and prevention of sudden death in conscious dogs with a healed myocardial infarction. Circulation Research 68, 1471–1481.

Yamazaki, T., Akiyama, T., Kitagawa, H., Takauchi, Y., Kawada, T., Sunagawa, K., 1997. A new, concise dialysis approach to assessment of cardiac sympathetic nerve terminal abnormalities. American Journal of Physiology. Heart and Circulatory Physiology 272, H1182–H1187.

Yamazaki, T., Akiyama, T., Mori, H., 2001. Effects of nociceptin on cardiac norepinephrine and acetylcholine release evoked by ouabain. Brain Research 904, 153–156.

Am J Physiol Heart Circ Physiol 291: H2187–H2191, 2006.
First published June 9, 2006; doi:10.1152/ajpheart.00175.2006.

Effects of Ca^{2+} channel antagonists on nerve stimulation-induced and ischemia-induced myocardial interstitial acetylcholine release in cats

Toru Kawada,[1] Toji Yamazaki,[2] Tsuyoshi Akiyama,[2] Kazunori Uemura,[1] Atsunori Kamiya,[1] Toshiaki Shishido,[1] Hidezo Mori,[2] and Masaru Sugimachi[1]

[1]Department of Cardiovascular Dynamics, Advanced Medical Engineering Center, National Cardiovascular Center Research Institute and [2]Department of Cardiac Physiology, National Cardiovascular Center Research Institute, Osaka, Japan

Submitted 17 February 2006; accepted in final form 7 June 2006

Kawada, Toru, Toji Yamazaki, Tsuyoshi Akiyama, Kazunori Uemura, Atsunori Kamiya, Toshiaki Shishido, Hidezo Mori, and Masaru Sugimachi. Effects of Ca^{2+} channel antagonists on nerve stimulation-induced and ischemia-induced myocardial interstitial acetylcholine release in cats. *Am J Physiol Heart Circ Physiol* 291: H2187–H2191, 2006. First published June 9, 2006; doi:10.1152/ajpheart.00175.2006.—Although an axoplasmic Ca^{2+} increase is associated with an exocytotic acetylcholine (ACh) release from the parasympathetic postganglionic nerve endings, the role of voltage-dependent Ca^{2+} channels in ACh release in the mammalian cardiac parasympathetic nerve is not clearly understood. Using a cardiac microdialysis technique, we examined the effects of Ca^{2+} channel antagonists on vagal nerve stimulation- and ischemia-induced myocardial interstitial ACh releases in anesthetized cats. The vagal stimulation-induced ACh release [22.4 nM (SD 10.6), $n = 7$] was significantly attenuated by local administration of an N-type Ca^{2+} channel antagonist ω-conotoxin GVIA [11.7 nM (SD 5.8), $n = 7$, $P = 0.0054$], or a P/Q-type Ca^{2+} channel antagonist ω-conotoxin MVIIC [3.8 nM (SD 2.3), $n = 6$, $P = 0.0002$] but not by local administration of an L-type Ca^{2+} channel antagonist verapamil [23.5 nM (SD 6.0), $n = 5$, $P = 0.758$]. The ischemia-induced myocardial interstitial ACh release [15.0 nM (SD 8.3), $n = 8$] was not attenuated by local administration of the L-, N-, or P/Q-type Ca^{2+} channel antagonists, by inhibition of Na^+/Ca^{2+} exchange, or by blockade of inositol 1,4,5-trisphosphate [Ins(1,4,5)P_3] receptor but was significantly suppressed by local administration of gadolinium [2.8 nM (SD 2.6), $n = 6$, $P = 0.0283$]. In conclusion, stimulation-induced ACh release from the cardiac postganglionic nerves depends on the N- and P/Q-type Ca^{2+} channels (with a dominance of P/Q-type) but probably not on the L-type Ca^{2+} channels in cats. In contrast, ischemia-induced ACh release depends on nonselective cation channels or cation-selective stretch activated channels but not on L-, N-, or P/Q type Ca^{2+} channels, Na^+/Ca^{2+} exchange, or Ins(1,4,5)P_3 receptor-mediated pathway.

cardiac microdialysis; ω-conotoxin GVIA; ω-conotoxin MVIIC; KB-R7943; verapamil; vagal stimulation

ALTHOUGH N-TYPE Ca^{2+} CHANNELS play a dominant role in norepinephrine release from sympathetic nerve endings (8, 33, 34), the type(s) of Ca^{2+} channels controlling ACh release in the mammalian parasympathetic system is not fully understood and show diversity among reports. To name a few, in isolated parasympathetic submandibular ganglia from the rat, neurotransmission is mediated by Ca^{2+} channels that are resistant to the L-, N-, P/Q-, and R- type Ca^{2+} channel antagonists (29). When the negative inotropic response to field stimulation was examined in the isolated guinea pig atria, Hong and Chang (8) reported the importance of P/Q-type Ca^{2+} channels, whereas Serone et al. (28) reported the importance of N-type Ca^{2+} channels. Because field stimulation in the isolated preparations could induce responses different from those in the in vivo conditions, we aimed to examine the effects of Ca^{2+} channel antagonists on the vagal nerve stimulation-induced myocardial interstitial ACh release in the in vivo feline heart.

Aside from the important role of the normal physiological regulation of the heart, the vagal nerve can be a therapeutic target for certain cardiovascular diseases (2, 3, 13, 22, 27). In previous studies, we have shown that acute myocardial ischemia causes myocardial interstitial ACh release in the ischemic region independently of efferent vagal nerve activity (12, 14). The comparison of the effects of Ca^{2+} channel antagonists on the ACh releases induced by vagal nerve stimulation and by acute myocardial ischemia may deepen our understanding about the ischemia-induced myocardial interstitial ACh release.

A cardiac microdialysis technique offers detailed analyses of in vivo myocardial interstitial ACh release (1, 15). Because the local administration of pharmacological agents through a dialysis probe can modulate ACh release without significantly affecting systemic hemodynamics, a combination of cardiac microdialysis with local pharmacological interventions is useful for analyzing the mechanisms of ACh release in vivo. In the present study, we examined the effects of Ca^{2+} channel antagonists on nerve stimulation- and ischemia-induced ACh releases in anesthetized cats. The results indicate that stimulation-induced ACh release from the cardiac parasympathetic postganglionic nerves depends on the N- and P/Q-type Ca^{2+} channels but probably not on the L-type Ca^{2+} channels. In contrast, ischemia-induced myocardial interstitial ACh release is resistant to the inhibition of L-, N-, and P/Q-type Ca^{2+} channels. In addition, the ischemia-induced myocardial ACh release is resistant to the inhibition of Na^+/Ca^{2+} exchanger and the blockade of inositol 1,4,5-trisphosphate [Ins(1,4,5)P_3] receptor but is suppressed by gadolinium, suggesting that nonselective cation channels or cation-selective stretch-activated channels are involved.

MATERIALS AND METHODS

Common Preparation

Animal care was provided in accordance with the *Guiding Principles for the Care and Use of Animals in the Field of Physiological*

Address for reprint requests and other correspondence: T. Kawada, Dept. of Cardiovascular Dynamics, Advanced Medical Engineering Center, National Cardiovascular Center Research Institute, 5-7-1 Fujishirodai, Suita, Osaka 565-8565, Japan (e-mail: torukawa@res.ncvc.go.jp).

The costs of publication of this article were defrayed in part by the payment of page charges. The article must therefore be hereby marked "*advertisement*" in accordance with 18 U.S.C. Section 1734 solely to indicate this fact.

Sciences approved by the Physiological Society of Japan. All protocols were approved by the Animal Subjects Committee of the National Cardiovascular Center. Adult cats weighing from 2.2 to 4.2 kg were anesthetized via an intraperitoneal injection of pentobarbital sodium (30–35 mg/kg) and ventilated mechanically with room air mixed with oxygen. The depth of anesthesia was maintained with a continuous intravenous infusion of pentobarbital sodium (1–2 mg·kg^{-1}·h^{-1}) through a catheter inserted from the right femoral vein. Systemic arterial pressure was monitored from a catheter inserted from the right femoral artery. The vagi were sectioned bilaterally at the neck. The esophageal temperature of the animal, which was measured by a thermometer (CTM-303, TERUMO, Japan), was maintained at around 37°C using a heated pad and a lamp.

With the animal in the lateral position, the left fifth and sixth ribs were resected to expose the heart. A dialysis probe was implanted transversely, using a fine guiding needle, into the anterolateral free wall of the left ventricle perfused by the left anterior descending coronary artery (LAD). Heparin sodium (100 U/kg) was administered intravenously to prevent blood coagulation. At the end of the experiment, the experimental animals were killed with an overdose of pentobarbital sodium. Postmortem examination confirmed that the dialysis probe had been threaded in the middle layer of the left ventricular myocardium. The thickness of the left ventricular free wall was ~7–8 mm, and the semipermeable membrane of the dialysis probe was positioned ~3–4 mm from the epicardial surface.

Dialysis Technique

The materials and properties of the dialysis probe have been described previously (1). Briefly, we designed a transverse dialysis probe. A dialysis fiber of semipermeable membrane (13 mm length, 310 μm OD, 200 μm ID; PAN-1200, 50,000 molecular weight cutoff, Asahi Chemical, Japan) was glued at both ends to polyethylene tubes (25 cm length, 500 μm OD, 200 μm ID). The dialysis probe was perfused at a rate of 2 μl/min with Ringer solution containing a cholinesterase inhibitor eserine (physostigmine, 100 μM). Experimental protocols were started 2 h after the dialysis probe was implanted when the ACh concentration in the dialysate reached a steady state. The ACh concentration in the dialysate was measured by high-performance liquid chromatography with electrochemical detection (Eicom, Kyoto, Japan).

Local administration of a pharmacological agent was carried out through a dialysis probe. That is to say, we added the pharmacological agent to the perfusate and allowed 1 h for a settling time. The pharmacological agent should spread around the semipermeable membrane, thereby affecting the neurotransmitter release in the vicinity of the semipermeable membrane. Because the distribution across the semipermeable membrane is required, based on previous results (33, 34), we used the pharmacological agent at the concentration 10–100 times higher than that required for complete channel blockade in experimental settings in vitro.

Specific Preparation and Protocols

Protocol 1. Bipolar platinum electrodes were attached bilaterally to the cardiac ends of the sectioned vagi at the neck. The nerves and electrodes were covered with warmed mineral oil for insulation. The vagal nerves were stimulated for 15 min (20 Hz, 1 ms, 10 V). We measured the stimulation-induced ACh release in the absence of Ca^{2+} channel blockade (control, $n = 7$) and examined the effects of an L-type Ca^{2+} channel antagonist verapamil (100 μM, $n = 5$), an N-type Ca^{2+} channel antagonist ω-conotoxin GVIA (10 μM, $n = 7$), a P/Q-type Ca^{2+} channel antagonist ω-conotoxin MVIIC (10 μM, $n = 6$), and combined administration of ω-conotoxin GVIA and ω-conotoxin MVIIC (10 μM each, $n = 6$).

Protocol 2. Because a preliminary result from *protocol 1* suggested that local administration of verapamil was ineffective in suppressing stimulation-induced ACh release, we examined the effects of the intravenous administration of verapamil (300 μg/kg, $n = 6$) on stimulation-induced ACh release in vagotomized animals as a supplemental experiment.

Protocol 3. A 60-min LAD occlusion was performed by using a 3-0 silk suture passed around the LAD just distal to the first diagonal branch. We measured the ACh levels during 45–60 min of ischemia in the absence of Ca^{2+} channel blockade (control, $n = 8$) and examined the effects of verapamil (100 μM, $n = 5$), ω-conotoxin GVIA (10 μM, $n = 5$), and ω-conotoxin MVIIC (10 μM, $n = 5$). A previous result indicated that the ischemia-induced ACh release reached the steady state during 45–60 min of ischemia (14). We also examined the effects of three additional agents, a Na^+/Ca^{2+} exchange inhibitor KB-R7943 (10 μM, $n = 5$) (9, 10), an Ins(1,4,5)P_3 receptor blocker xestospongin C (500 μM, $n = 6$) (25), and a nonselective cation channel blocker or a cation-selective stretch activated channel blocker gadolinium (1 mM) (5, 17), on the ischemia-induced ACh release.

Statistical Analysis

All data are presented as mean (SD) values. In *protocol 1*, we compared stimulation-induced ACh release among the five groups using one-way analysis of variance followed by the Student-Neuman-Keuls test (6). In *protocol 2*, we used an unpaired-*t* test (two-sided) to examine the effect of intravenous verapamil administration on stimulation-induced ACh release. In *protocol 3*, we compared ischemia-induced ACh release among the seven groups using one-way analysis of variance followed by the Dunnett' test against the control. For all analyses, differences were considered significant when $P < 0.05$.

RESULTS

In *protocol 1*, the ACh level during electrical vagal stimulation was 22.4 nM (SD 10.6). Local administration of verapamil did not affect stimulation-induced ACh release (Fig. 1). In contrast, local administration of ω-conotoxin GVIA or ω-conotoxin MVIIC suppressed stimulation-induced ACh release. The extent of suppression was greater in the latter. The ACh level was significantly lower in the simultaneous administration group (ω-conotoxin GVIA + ω-conotoxin MVIIC)

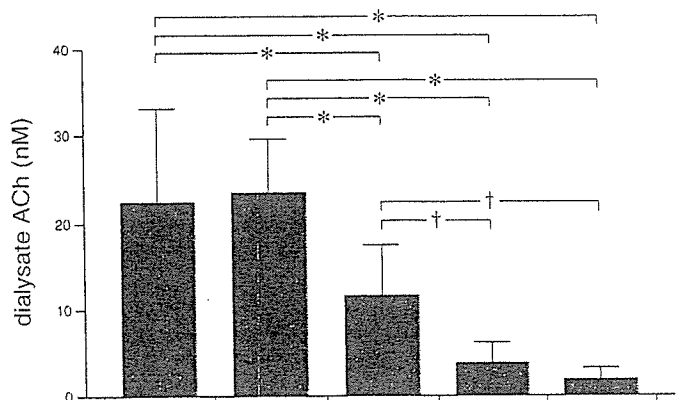

	vehicle	verapamil	ω-CTX GVIA	ω-CTX MVIIC	ω-CTX MVIIC + ω-CTX GVIA
vehicle		0.758	*0.0054*	*0.0002*	*0.0002*
verapamil	0.758		*0.0068*	*0.0002*	*0.0001*
GVIA	*0.0054*	*0.0068*		*0.033*	*0.025*
MVIIC	*0.0002*	*0.0002*	*0.033*		0.581
MVIIC+GVIA	*0.0002*	*0.0001*	*0.025*	0.581	

Fig. 1. Effects of local administration of verapamil, ω-conotoxin GVIA, ω-conotoxin MVIIC, or ω-conotoxin GVIA plus ω-conotoxin MVIIC on vagal nerve stimulation-induced myocardial interstitial ACh release. Both ω-conotoxin GVIA and ω-conotoxin MVIIC, but not verapamil, suppressed stimulation-induced ACh release. Data are mean (SD) values. *$P < 0.01$, †$P < 0.05$. The exact P values are presented.

than that in the ω-conotoxin GVIA group but was not different from the ω-conotoxin MVIIC group.

In *protocol 2*, the intravenous administration of verapamil did not significantly change stimulation-induced ACh release [21.7 nM (SD 12.8)] compared with the control group (P = 0.91).

In *protocol 3*, the ACh level in the ischemic region was 14.9 nM (SD 8.3) during 45–60 min of acute myocardial ischemia. Inhibition of voltage-dependent Ca^{2+} channels by local administration of verapamil, ω-conotoxin GVIA, or ω-conotoxin MVIIC did not affect ischemia-induced ACh release (Fig. 2). Inhibition of the reverse mode action of Na^+/Ca^{2+} exchange by local administration of KB-R7943 appeared to have augmented rather than suppressed ischemia-induced ACh release, though there was no statistically significant difference from the control. Blockade of the Ins(1,4,5)P_3 receptor by local administration of xestospongin C did not affect the ischemia-induced ACh release. In contrast, blockade of nonselective cation channels or cation-selective stretch-activated channels by local administration of gadolinium suppressed the ischemia-induced ACh release.

DISCUSSION

Ca^{2+} Channels Involved in Stimulation-Induced ACh Release

Although neurotransmitter release at mammalian sympathetic neuroeffector junctions predominantly depends on Ca^{2+} influx through N-type Ca^{2+} channels (23, 33, 34), the type(s) of Ca^{2+} channels involved in ACh release from cardiac parasympathetic neuroeffector junctions show diversity among reports (8, 28). One possible factor hampering investigations into parasympathetic postganglionic neurotransmitter release in response to vagal nerve stimulation in vivo is that the parasympathetic ganglia are usually situated in the vicinity of the effector organs, thereby making it difficult to separately assess ACh release from preganglionic and postganglionic nerves. In the previous study from our laboratory, intravenous administration, but not local administration of a ganglionic blocker, hexamethonium reduced vagal stimulation-induced ACh release assessed by cardiac microdialysis (1). The negligible effect of local hexamethonium administration on stimulation-induced ACh release suggests the lack of parasympathetic ganglia around the dialysis probe. In support of our speculation, a recent neuroanatomical finding indicates that three ganglia, away from the left anterior free wall targeted by the dialysis probe, provide the major source for left ventricular postganglionic innervation in cats: a cranioventricular ganglion, a left ventricular ganglion 2 (so designated), and an interventriculo-septal ganglion (11). Therefore, ACh, as measured by cardiac microdialysis, is considered to predominantly reflect ACh release from parasympathetic postganglionic nerves.

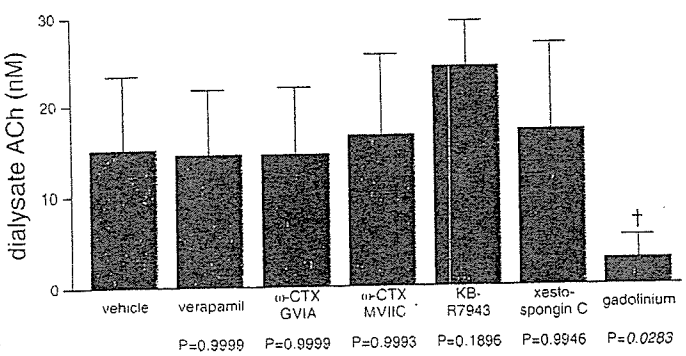

Fig. 2. Effects of local administration of verapamil, ω-conotoxin GVIA, ω-conotoxin MVIIC, KB-R7943, xestospongin C, or gadolinium on acute myocardial ischemia-induced myocardial interstitial ACh release in the ischemic region. Gadolinium alone suppressed the ischemia-induced ACh release. Data are mean (SD) values. †P < 0.05. The exact P values are presented.

Local (*protocol 1*) or intravenous (*protocol 2*) administration of verapamil did not affect stimulation-induced ACh release. In contrast, vagal stimulation-induced ACh release was reduced in both the ω-conotoxin GVIA and ω-conotoxin MVIIC groups but to a greater extent in the latter (Fig. 1). Therefore, both N- and P/Q-type, but probably not L-type, Ca^{2+} channels are involved in stimulation-induced ACh release from the cardiac parasympathetic postganglionic nerves in cats. The contribution of P/Q type Ca^{2+} channels to ACh release might be greater than that of N-type Ca^{2+} channels. Hong and Chang (8) reported that the negative inotropic response to field stimulation depends predominantly on the P/Q-type Ca^{2+} channels in isolated guinea pig atria, whereas Serone et al. (28) reported the predominance of N-type Ca^{2+} channels. In those studies, the field stimulation employed differed from ordinary activation of the postganglonic nerves by nerve discharge and, in addition, ACh release was not directly measured. The present study directly demonstrated the involvement of P/Q- and N-type Ca^{2+} channels in the stimulation-induced ACh release in the cardiac parasympathetic postganglionic nerves. These results support the concept that multiple subtypes of the voltage-gated Ca^{2+} channel mediate transmitter release from the same population of parasympathetic neurons (31).

Stimulation-induced ACh release was suppressed by ~50% in the ω-conotoxin GVIA group and by ~80% in the ω-conotoxin MVIIC group. The algebraic summation of the extent of suppression exceeded 100%. The phenomenon may be in part due to the nonlinear dose-response relationship between Ca^{2+} influx and transmitter release (32). The supra-additive phenomenon may be also due to the affinity of ω-conotoxin MVIIC to N-type Ca^{2+} channels (8, 26, 36). Combined local administration of ω-conotoxin GVIA and ω-conotoxin MVIIC almost completely suppressed stimulation-induced ACh release to a level similar to that achieved by the Na^+ channel inhibitor tetrodotoxin (15). Therefore, involvement of another untested type of Ca^{2+} channel(s) is unlikely in the stimulation-induced ACh release from the cardiac parasympathetic postganglionic nerves in cats.

Ca^{2+} Channels and Ischemia-Induced ACh Release

In a previous study, we showed that acute myocardial ischemia evokes myocardial interstitial ACh release in the ischemic region via a local mechanism independent of efferent vagal nerve activity (14). In that study, the inhibition of intracellular Ca^{2+} mobilization by local administration of 3,4,5-trimethoxybenzoic acid 8-(diethyl amino)-octyl ester (TMB-8) suppressed ischemia-induced ACh release, suggesting that an axoplasmic Ca^{2+} elevation is essential for the ischemia-induced ACh release. Because tissue K^+ concentration increases in the ischemic region (7, 18), high K^+-induced

depolarization could activate voltage-dependent Ca^{2+} channels even in the absence of efferent vagal nerve activity. However, ischemia-induced ACh release was not suppressed by local administration of verapamil, ω-conotoxin GVIA, or ω-conotoxin MVIIC (Fig. 2). Therefore, Ca^{2+} entry through the voltage-dependent Ca^{2+} channels is unlikely a mechanism for the ischemia-induced myocardial interstitial ACh release.

Acute myocardial ischemia causes energy depletion in the ischemic region, which impairs Na^+-K^+-ATPase activity. Ischemia also causes acidosis in the ischemic region, which promotes Na^+/H^+ exchange. As a result, ischemia causes intracellular Na^+ accumulation. The decrease in the Na^+ gradient across the plasma membrane may then cause the Na^+/Ca^{2+} exchanger to operate in the reverse mode, facilitating intracellular Ca^{2+} overload. KB-R7943 can inhibit the reverse mode of Na^+/Ca^{2+} exchange (9, 10) and its potential to protect against ischemia-reperfusion injury has been reported (21). In the present study, however, local administration of KB-R7943 failed to suppress and rather increased ACh release during ischemia as opposed to our expectation. It is plausible that the inhibition of reverse mode of Na^+/Ca^{2+} may have facilitated the accumulation of intracellular Na^+ and induced adverse effects that cancelled the possible beneficial effects derived from the inhibition of Ca^{2+} entry through the Na^+/Ca^{2+} exchanger itself. In addition, KB-R7943 could inhibit the forward mode of Na^+/Ca^{2+} exchange and reduce Ca^{2+} efflux (16), contributing to the intracellular Ca^{2+} accumulation and ACh release. In the present study, we observed the effects of KB-R7943 only during the ischemic period. However, accumulation of intracellular Na^+ through Na^+/H^+ exchange is enhanced on reperfusion due to the washout of extracellular H^+ (20). The inhibition of Na^+/Ca^{2+} exchange to suppress Ca^{2+} overload might become more important during the reperfusion phase. For instance, the percent segment shortening of the left ventricle was improved by KB-R7943 during reperfusion but not during ischemia (35).

As already mentioned, the ischemia-induced ACh release can be blocked by TMB-8 and thus the intracellular Ca^{2+} mobilization is required for the ischemia-induced ACh release (14). Besides the Ca^{2+} entries through voltage-dependent Ca^{2+} channels and via the reverse mode of Na^+/Ca^{2+} exchanger, Ca^{2+} may be mobilized from the endoplasmic reticulum via pathological pathways. As an example, the mitochondrial permeability transition pore triggered in pathological conditions is linked to cytochrome *c* release. Cytochrome *c* can bind to the endoplasmic reticulum Ins(1,4,5)P_3 receptor, rendering the channel insensitive to autoinhibition by high cytosolic Ca^{2+} concentration and resulting in enhanced endoplasmic reticulum Ca^{2+} release (4, 30). In the present study, however, blockade of Ins(1,4,5)P_3 receptor by xestospongin C failed to suppress the ischemia-induced ACh release. In contrast, local administration of gadolinium significantly suppressed the ischemia-induced ACh release. Therefore, nonselective cation channels or cation-selective stretch-activated channels contribute to the ischemia-induced ACh release. During myocardial ischemia, the ischemic region can be subjected to paradoxical systolic bulging. Such bulging likely opens stretch-activated channels and causes myocardial interstitial ACh release, possibly leading to cardioprotection by ACh against ischemic injury (2).

Limitations

First, the experiment was performed under anesthetic conditions, which may have influenced basal autonomic activity. However, because we sectioned the vagi at the neck, basal autonomic activity may have had only a minor effect on ACh release during the vagal stimulation and during acute myocardial ischemia. Second, we added eserine to the perfusate to inhibit immediate degradation of ACh (24), which may have increased the ACh level in the synaptic cleft and activated regulatory pathways such as autoinhibition of ACh release via muscarinic receptors (24). However, the myocardial interstitial ACh level measured under this condition could reflect changes induced by Na^+ channel inhibitor, choline uptake inhibitor, and vesicular ACh transport inhibitor as described in a previous study (15). Therefore, we think that the interpretation of the present results is reasonable. Third, tissue and species differences should be taken into account when extrapolating the present findings, because significant heterogeneity in the Ca^{2+} channels involved in the mammalian parasympathetic system may exist. Finally, we used verapamil to test the involvement of L-type Ca^{2+} channels in the ACh release. There are three major types of L-type Ca^{2+} channel antagonists with different binding domains (verapamil, nifedipine, and diltiazem) (19). Whether the effects on the ACh release are common among the three types of L-type Ca^{2+} channel antagonists remains unanswered.

In conclusion, the N- and P/Q-type Ca^{2+} channels (with the P/Q-type dominant), but probably not the L-type Ca^{2+} channels, are involved in vagal stimulation-induced ACh release from the cardiac parasympathetic postganglionic nerves in cats. In contrast, myocardial interstitial ACh release in the ischemic myocardium is resistant to the blockade of L-, N-, and P/Q-type Ca^{2+} channels. In addition, the ischemia-induced myocardial ACh release is resistant to the inhibition of Na^+/Ca^{2+} exchanger and the blockade of Ins(1,4,5)P_3 receptor but is suppressed by gadolinium, suggesting that nonselective cation channels or cation-selective stretch-activated channels are involved.

GRANTS

This study was supported by Health and Labour Sciences Research Grant for Research on Advanced Medical Technology from the Ministry of Health, Labour and Welfare of Japan, Health and Labour Sciences Research Grant for Research on Medical Devices for Analyzing, Supporting and Substituting the Function of Human Body from the Ministry of Health, Labour and Welfare of Japan, Health and Labour Sciences Research Grant H18-Iryo-Ippan-023 from the Ministry of Health, Labour and Welfare of Japan, Program for Promotion of Fundamental Studies in Health Science from the National Institute of Biomedical Innovation, a Grant provided by the Ichiro Kanehara Foundation, Ground-based Research Announcement for Space Utilization promoted by Japan Space Forum, and Industrial Technology Research Grant Program in 03A47075 from New Energy and Industrial Technology Development Organization of Japan.

REFERENCES

1. **Akiyama T, Yamazaki T, and Ninomiya I.** In vivo detection of endogenous acetylcholine release in cat ventricles. *Am J Physiol Heart Circ Physiol* 266: H854–H860, 1994.
2. **Ando M, Katare RG, Kakinuma Y, Zhang D, Yamasaki F, Muramoto K, and Sato T.** Efferent vagal nerve stimulation protects heart against ischemia-induced arrhythmias by preserving connexin43 protein. *Circulation* 112: 164–170, 2005.

3. **Bibevski S and Dunlap ME.** Prevention of diminished parasympathetic control of the heart in experimental heart failure. *Am J Physiol Heart Circ Physiol* 287: H1780–H1785, 2004.
4. **Brookes PS, Yoon Y, Robotham JL, Anders MW, and Sheu SS.** Calcium, ATP, and ROS: a mitochondrial love-hate triangle. *Am J Physiol Cell Physiol* 287: C817–C833, 2004.
5. **Caldwell RA, Clemo HF, and Baumgarten CM.** Using gadolinium to identify stretch-activated channels: technical considerations. *Am J Physiol Cell Physiol* 275: C619–C621, 1998.
6. **Glantz SA.** *Primer of Biostatistics* (5th ed) New York: McGraw-Hill, 2002.
7. **Hirche HJ, Franz CHR, Bös L, Bissig R, Lang R, and Schramm M.** Myocardial extracellular K^+ and H^+ increase and noradrenaline release as possible cause of early arrhythmias following acute coronary artery occlusion in pigs. *J Mol Cell Cardiol* 12: 579–593, 1979.
8. **Hong SJ and Chang CC.** Calcium channel subtypes for the sympathetic and parasympathetic nerves of guinea-pig atria. *Br J Pharmacol* 116: 1577–1582, 1995.
9. **Iwamoto T, Kita S, Uehara A, Inoue Y, Taniguchi Y, Imanaga I, and Shigekawa M.** Structural domains influencing sensitivity to isothiourea derivative inhibitor KB-R7943 in cardiac Na^+/Ca^{2+} exchanger. *Mol Pharmacol* 59: 524–531, 2001.
10. **Iwamoto T, Watano T, and Shigekawa M.** A novel isothiourea derivative selectively inhibits the reverse mode of Na^+/Ca^{2+} exchange in cells expressing NCX1. *J Biol Chem* 271: 22391–22397, 1996.
11. **Johnson TA, Gray AL, Lauenstein JM, Newton SS, and Massari VJ.** Parasympathetic control of the heart. I. An interventriculo-septal ganglion is the major source of the vagal intracardiac innervation of the ventricles. *J Appl Physiol* 96: 2265–2272, 2004.
12. **Kawada T, Yamazaki T, Akiyama T, Inagaki M, Shishido T, Zheng C, Yanagiya Y, Sugimachi M, and Sunagawa K.** Vagosympathetic interactions in ischemia-induced myocardial norepinephrine and acetylcholine release. *Am J Physiol Heart Circ Physiol* 280: H216–H221, 2001.
13. **Kawada T, Yamazaki T, Akiyama T, Li M, Ariumi H, Mori H, Sunagawa K, and Sugimachi M.** Vagal stimulation suppresses ischemia-induced myocardial interstitial norepinephrine release. *Life Sci* 78: 882–887, 2006.
14. **Kawada T, Yamazaki T, Akiyama T, Sato T, Shishido T, Inagaki M, Takaki H, Sugimachi M, and Sunagawa K.** Differential acetylcholine release mechanisms in the ischemic and non-ischemic myocardium. *J Mol Cell Cardiol* 32: 405–414, 2000.
15. **Kawada T, Yamazaki T, Akiyama T, Shishido T, Inagaki M, Uemura K, Miyamoto T, Sugimachi M, Takaki H, and Sunagawa K.** In vivo assessment of acetylcholine-releasing function at cardiac vagal nerve terminals. *Am J Physiol Heart Circ Physiol* 281: H139–H145, 2001.
16. **Kimura J, Watano T, Kawahara M, Sakai E, and Yatabe J.** Direction-independent block of bi-directional Na^+/Ca^{2+} exchange current by KB-R7943 in guinea-ping cardiac myocytes. *Br J Pharmacol* 128: 969–974, 1999.
17. **Kimura S, Mieno H, Tamaki K, Inoue M, and Chayama K.** Nonselective cation channel as a Ca^{2+} influx pathway in pepsinogen-secreting cells of bullfrog esophagus. *Am J Physiol Gastrointest Liver Physiol* 281: G333–G341, 2001.
18. **Kléber AG.** Extracellular potassium accumulation in acute myocardial ischemia. *J Mol Cell Cardiol* 16: 389–394, 1984.
19. **Kurokawa J, Adachi-Akahane S, and Nagao T.** 1-5-Benzothiazepine binding domain is located on the extracellular side of the cardiac L-type Ca^{2+} channel. *Mol Pharmacol* 51: 262–268, 1997.
20. **Lazdunski M, Frelin C, and Vigne P.** The sodium/hydrogen exchange system in cardiac cells: its biochemical and pharmacological properties and its role in regulating internal concentrations of sodium and internal pH. *J Mol Cell Cardiol* 17: 1029–1042, 1985.
21. **Lee C, Dhalla NS, and Hryshko LV.** Therapeutic potential of novel Na^+-Ca^{2+} exchange inhibitors in attenuating ischemia-reperfusion injury. *Can J Cardiol* 21: 509–516, 2005.
22. **Li M, Zheng C, Sato T, Kawada T, Sugimachi M, and Sunagawa K.** Vagal nerve stimulation markedly improves long-term survival after chronic heart failure in rats. *Circulation* 109: 120–124, 2004.
23. **Molderings GJ, Likungu J, and Göthert M.** N-type calcium channels control sympathetic neurotransmission in human heart atrium. *Circulation* 101: 403–407, 2000.
24. **Nicholls DG.** *Proteins, Transmitters and Synapses*. Oxford: Blackwell Science, 1994.
25. **Oka T, Sato K, Hori M, Ozaki H, and Karaki H.** Xestospongin C, a novel blocker of IP_3 receptor, attenuates the increase in cytosolic calcium level and degranulation that is induced by antigen in RBL-2H3 mast cells. *Br J Pharmacol* 135: 1959–1966, 2002.
26. **Randall A and Tsien RW.** Pharmacological dissection of multiple types of Ca^{2+} channel currents in rat cerebellar granule neurons. *J Neurosci* 15: 2995–3012, 1995.
27. **Schauerte P, Scherlag BJ, Scherlag MA, Goli S, Jackman WM, and Lazzara R.** Ventricular rate control during atrial fibrillation by cardiac parasympathetic nerve stimulation: a transvenous approach. *J Am Coll Cardiol* 34: 2043–2050, 1999.
28. **Serone AP and Angus JA.** Role of N-type calcium channels in autonomic neurotransmission in guinea-pig isolated left atria. *Br J Pharmacol* 127: 927–934, 1999.
29. **Smith AB, Motin L, Lavidis NA, and Adams DJ.** Calcium channels controlling acetylcholine release from preganglionic nerve terminals in rat autonomic ganglia. *Neuroscience* 95: 1121–1127, 2000.
30. **Verkhratsky A and Toescu EC.** Endoplasmic reticulum Ca^{2+} homeostasis and neuronal death. *J Cell Mol Med* 4: 351–361, 2003.
31. **Waterman SA.** Multiple subtypes of voltage-gated calcium channel mediate transmitter release from parasympathetic neurons in the mouse bladder. *J Neurosci* 16: 4155–4161, 1996.
32. **Wheeler DB, Randall A, and Tsien RW.** Changes in action potential duration after reliance of excitatory synaptic transmission on multiple types of Ca^{2+} channels in rat hippocampus. *J Neurosci* 16: 2226–2237, 1996.
33. **Yahagi N, Akiyama T, and Yamazaki T.** Effects of ω-conotoxin GVIA on cardiac sympathetic nerve function. *J Auton Nerv Syst* 68: 43–48, 1998.
34. **Yamazaki T, Akiyama T, Kitagawa H, Takauchi Y, Kawada T, and Sunagawa K.** A new, concise dialysis approach to assessment of cardiac sympathetic nerve terminal abnormalities. *Am J Physiol Heart Circ Physiol* 272: H1182–H1187, 1997.
35. **Yoshitomi O, Akiyama D, Hara T, Cho S, Tomiyasu S, and Sumikawa K.** Cardioprotective effects of KB-R7943, a novel inhibitor of Na^+/Ca^{2+} exchanger, on stunned myocardium in anesthetized dogs. *J Anesth* 19: 124–130, 2005.
36. **Zhang JF, Randall AD, Ellinor PT, Horne WA, Sather WA, Tanabe T, Schwarz TL, and Tsien RW.** Distinctive pharmacology and kinetics of cloned neuronal Ca^{2+} channels and their possible counterparts in mammalian CNS neurons. *Neuropharmacology* 32: 1075–1088, 1993.

Laboratory Investigation

A New Protocol for Quantifying CD34+ Cells

in Peripheral Blood of Patients with Cardiovascular Disease

Akie Kikuchi-Taura
Toshihiro Soma, MD
Tomohiro Matsuyama, MD
David M. Stern, MD
Akihiko Taguchi, MD

Increasing evidence points to a role for circulating CD34-positive (CD34+) cells in vascular maintenance and neovascularization. Although there are established methods for evaluating absolute numbers of CD34+ cells in bone marrow or mobilized peripheral blood, there is no convenient and highly reproducible method for quantifying low numbers of CD34+ cells in blood samples, such as those from the peripheral blood of patients with cardiovascular disease. With current commonly used methods, the mean percentage of CD34+ cells in leukocyte fractions from such patients was only 0.02%, and the cumulative intra-assay coefficient of variation was ~30%. With use of the protocol described herein, actual counts of CD34+ cells increased ~5-fold and cumulative intra-assay coefficients of variation were reduced to ~7%. The new method is useful to precisely measure low numbers of CD34+ cells in samples, and it has potential as a screening tool to evaluate cardiovascular risk in large patient populations. ***(Tex Heart Inst J 2006;33:427-9)***

Key words: *Antigens, CD34/analysis; blood cell count; cardiovascular diseases; cell sorter, fluorescence-activated; CD34-positive cells; coefficients of variation; endothelium, vascular/cytology; stem cells*

From: *Department of Clinical Laboratory (Ms Kikuchi-Taura and Dr. Soma), National Hospital Organization, Osaka Minami Medical Center, Osaka 586-8521, Japan; Department of Internal Medicine (Dr. Matsuyama), Hyogo College of Medicine, Hyogo 663-8501, Japan; College of Medicine (Dr. Stern), University of Cincinnati, Cincinnati, Ohio 45221; and Department of Cerebrovascular Disease (Dr. Taguchi), National Cardiovascular Center, Osaka 565-8565, Japan*

This work was supported by a Grant-in-Aid for Scientific Research from the Ministry of Health, Labor, and Welfare, Japan.

Address for reprints: *Akihiko Taguchi, MD, Department of Cerebrovascular Disease, National Cardiovascular Center, 5-7-1 Fujishiro-dai, Suita, Osaka 565-8565, Japan*

E-mail: ataguchi@res.ncvc.go.jp

In vasculature maintenance and neovascularization, there is increasing evidence of a role for circulating endothelial progenitor cells (EPCs)—including the populations of CD34-positive (CD34+) cells that are present in peripheral blood.[1] As a source of numerous growth and angiogenesis factors at ischemic loci, CD34+ cells also contribute to vascular homeostasis.[2] Furthermore, initial clinical trials of cell transplantation in treating ischemia of the hind limb[3] and myocardium[4] have shown promising results. On the basis of these observations, circulating EPCs[5] and CD34+ cells[6] have been evaluated in patients with cardiovascular disease, and strong correlations of their levels with vascular function have been reported. However, procedures to evaluate EPCs and CD34+ cells are not simple[5]; because of low numbers of circulating CD34+ cells, routine FACS (fluorescence-activated cell sorter) analysis[7] of CD34+ cell counts in patients with cardiovascular disease is not feasible. In this report, we demonstrate a new method that facilitates determination of the absolute number of circulating CD34+ cells in patients with low levels of CD34+ cells.

Patients and Methods

This study was approved by the Human Assurance Committee of the National Cardiovascular Center and Osaka Minami Medical Center, and all subjects provided written informed consent. Results of experiments are reported as mean ± standard error.

Analysis of Peripheral Blood

Three milliliters of heparinized peripheral blood were obtained from 20 patients who had histories of cardiovascular disease: 14 had sustained myocardial infarction, and 9 had sustained cerebral infarction (3 had histories of both). Patients who had experienced vascular events within 30 days of measurement were excluded. The study group included 12 men and 8 women, with a mean age of 74 ± 1.7 years (range, 59–87 yr). Medicines taken by study subjects included anticoagulants (aspirin, 17); antihypertensive agents, including calcium-channel antagonists, angiotensin-converting enzyme (ACE) inhibitors, or both (14); and sulfonylureas for glycemic control (5). Patients who were taking HMG-CoA reductase inhibitors (statins) were excluded from the study.

First, we counted circulating CD34+ cells with ProCount™ (BD Bioscience; San Jose, Calif) and Stem-Kit™ (Beckman Coulter; Marseilles, France), according to the